Journal Pre-proof



Advances in preclinical tissue engineering strategies for bladder reconstruction: a systematic review.

Laura Giacomel, Irene Paraboschi, Ugo Maria Pierucci, Michela Marinaro, Marco Paciotti, Vittorio Fasulo, Giovanni Lughezzani, Massimo Garriboli, Nicolò Maria Buffi, Silvia Farè, Gloria Pelizzo

PII: S0022-3468(26)00646-9

DOI: https://doi.org/10.1016/j.jpedsurg.2026.163564

Reference: YJPSU 163564

To appear in: *Journal of Pediatric Surgery*

Received Date: 10 February 2026

Revised Date: 25 July 2026

Accepted Date: 19 October 2026

Please cite this article as: Giacomel L, Paraboschi I, Pierucci UM, Marinaro M, Paciotti M, Fasulo V, Lughezzani G, Garriboli M, Buffi NM, Farè S, Pelizzo G, Advances in preclinical tissue engineering strategies for bladder reconstruction: a systematic review., *Journal of Pediatric Surgery*, https://doi.org/10.1016/j.jpedsurg.2026.163564.

This is a PDF of an article that has undergone enhancements after acceptance, such as the addition of a cover page and metadata, and formatting for readability. This version will undergo additional copyediting, typesetting and review before it is published in its final form. As such, this version is no longer the Accepted Manuscript, but it is not yet the definitive Version of Record; we are providing this early version to give early visibility of the article. Please note that Elsevier's sharing policy for the Published Journal Article applies to this version, see: https://www.elsevier.com/about/policies-and-standards/sharing#4-published-journal-article. Please also note that, during the production process, errors may be discovered which could affect the content, and all legal disclaimers that apply to the journal pertain.

Crown Copyright © 2026 Published by Elsevier Inc. All rights are reserved, including those for text and data mining, AI training, and similar technologies.

Journal Pre-proof

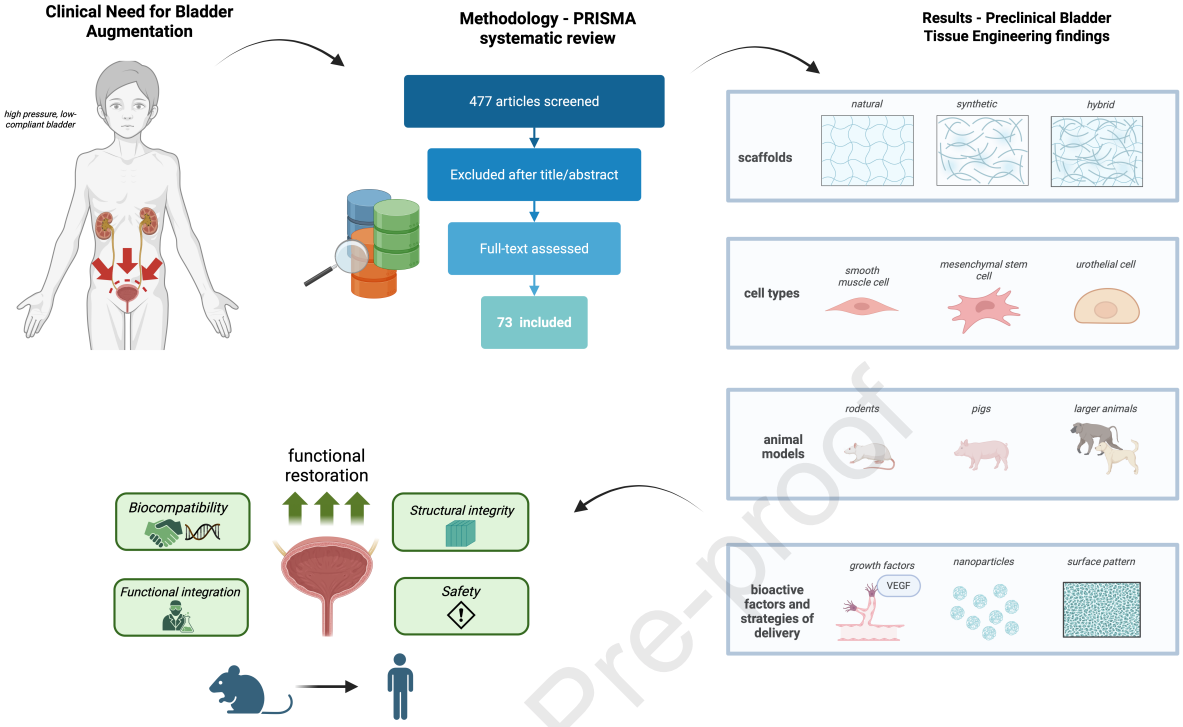
Advances in preclinical tissue engineering strategies for bladder reconstruction: a systematic review.

Laura Giacomel[1], Irene Paraboschi[1,2*], Ugo Maria Pierucci[1], Michela Marinaro[1], Marco Paciotti[3,4], Vittorio Fasulo[3,4], Giovanni Lughezzani[3,4], Massimo Garriboli[5], Nicolò Maria Buffi[3,4], Silvia Farè[6], Gloria Pelizzo[1,2].

1. Department of Pediatric Surgery, "Vittore Buzzi" Children's Hospital, Milano, Italy
2. Department of Biomedical and Clinical Science, University of Milano, Milano, Italy
3. Department of Urology, IRCCS Humanitas Research Hospital, Milano, Italy
4. Department of Biomedical Sciences, Humanitas University, Milano, Italy
5. Department of Paediatric Nephro-Urology, Evelina London Children's Hospital, Guy's and St. Thomas' NHS Foundation Trust, Westminster Bridge Rd, London, United Kingdom
6. Department of Chemistry Materials and Chemical Engineering, Politecnico di Milano, Milan, Italy

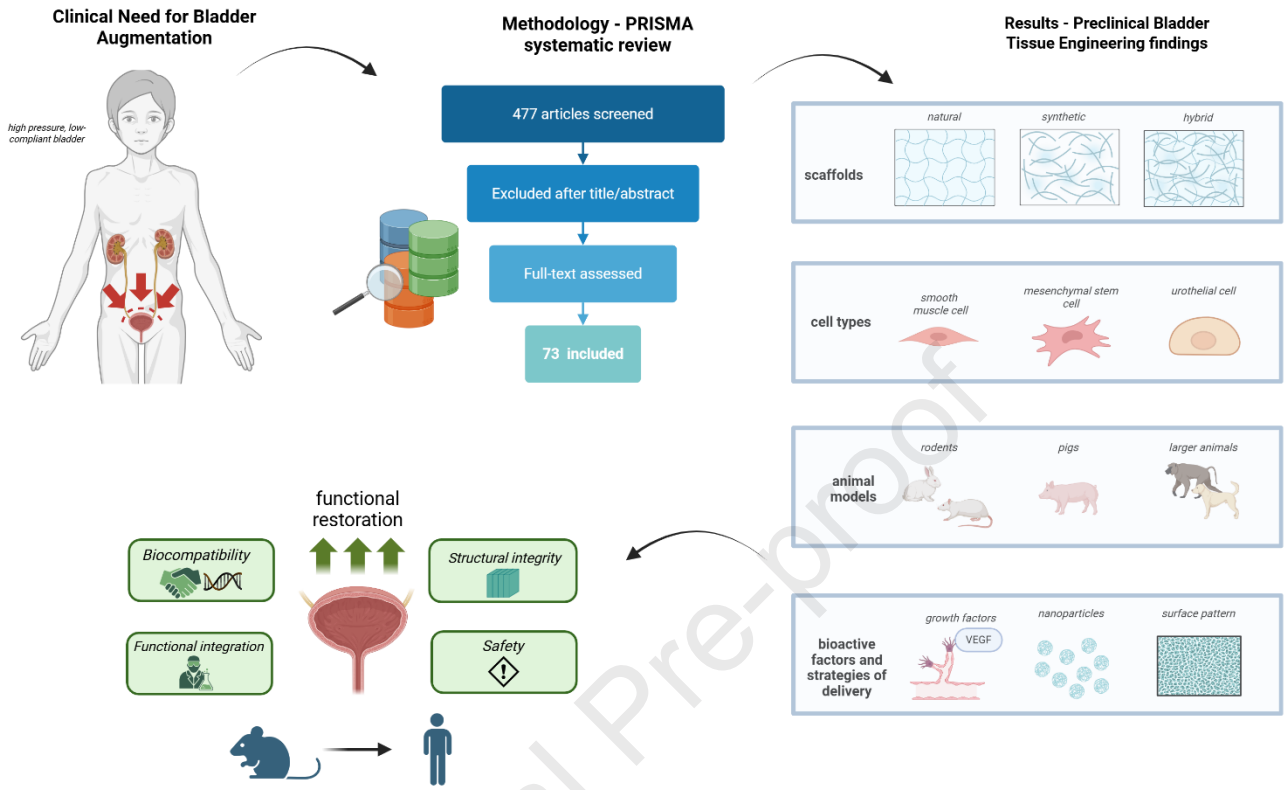
* Corresponding author:
Irene Paraboschi, MD
Department of Pediatric Surgery
"Vittore Buzzi" Children's Hospital
Milano, Italy
Department of Biomedical and Clinical Science
University of Milano
Milano, Italy
irene.paraboschi@unimi.it
Tel: +39.331.3229495

Journal Pre-proof



Journal Pre-proof

Abstract



Introduction: Bladder reconstruction remains challenging in pediatric patients needing augmentation cystoplasty for congenital anomalies, malignancies, or trauma. This review synthesizes *in vitro* and *in vivo* evidence on tissue-engineering strategies for pediatric bladder reconstruction.

Materials and methods: PRISMA guidelines were followed. PubMed, Scopus, and Embase were searched from inception to May 2025. Eligible studies investigated bioengineered constructs for pediatric bladder reconstruction and reported histological, molecular, or functional outcomes. Two reviewers independently performed study selection and data extraction, resolving disagreements by consensus.

Results: Seventy-three studies met inclusion criteria. Natural polymeric scaffolds predominated (61.6%), followed by synthetic (20.5%) and hybrid scaffolds (17.8%). Functionalization included VEGF, IGF-1, bFGF, surface patterning, and nanoparticles. Among cell-seeded studies (n=44), mesenchymal stem cells predominated, followed by urothelial cells, smooth muscle cells, and co-cultures. Among 54 *in vivo* studies, models included rodents (n=30), rabbits (n=10), pigs (n=9), dogs

Journal Pre-proof

(n=4), baboons (n=1), chicken embryos (n=1). Categories overlapped, as one study included both rats and pigs. Urothelial and smooth muscle regeneration was reported in all *in vivo* studies, angiogenesis in 90.7%. Functional bladder capacity was assessed in 34 studies, mainly in acellular scaffolds. Natural scaffolds supported regeneration, whereas synthetic scaffolds often required natural components; hybrid scaffolds showed variable integration. Immune responses were mild with natural ECM-based scaffolds, moderate with hybrids, and prolonged with synthetics. Thirty studies reported complications.

Conclusion: Durable functional regeneration appears dependent on integrated scaffold designs combining mechanical support, ECM-derived bioactivity, and biological cues. Composite and biofunctionalized scaffolds yielded consistent results, but large-animal studies remain essential for clinical translation.

Keywords: tissue engineering, augmentation cystoplasty, bladder replacement, bladder exstrophy, cloacal exstrophy.

Journal Pre-proof

Introduction

Bladder reconstruction remains a pivotal yet challenging surgical intervention in pediatric urology, primarily indicated for children affected by congenital or acquired disorders that severely compromise bladder structure and/or function. The most common underlying pathologies include posterior urethral valves, bladder exstrophy, neurogenic bladder, and sequelae of oncological resections [1].

In such patients, the bladder is frequently small, hypertonic, and low-compliant. This results in high intravesical pressures that are transmitted to the upper urinary tract, leading over time to progressive renal deterioration [1] [2]. Bladder augmentation is therefore reconstructive because it increases bladder capacity and compliance, and preventive because reducing storage pressure helps limit upper urinary tract deterioration and preserve renal function.

The current gold standard strategy is represented by an enterocystoplasty, where a segment of the gastrointestinal tract (most often ileum, but also colon or stomach), is used to enlarge the native bladder [1]. While effective from a mechanical standpoint, this approach is associated with major constraints and long-term complications, including metabolic disturbances, urinary tract infections, urolithiasis, and malignant disease [1]. The native bladder and the intestinal tissue fundamentally differ both at the inner layer where an epithelium is present instead of the specialized urothelium and at the muscular level, limiting functional integration and, almost inevitably, necessitating lifelong intermittent catheterization for achieving adequate emptying [1].

Given the limitations of the currently available reconstruction approaches, there is a profound need for bladder substitutes that are biocompatible, non-secretory, mechanically compliant, and capable of replicating native tissue structure and function. Tissue engineering offers a promising alternative, combining biomaterials as scaffolds, cells, and bioactive factors to recapitulate bladder tissue with near-native properties [1] [2] and promote bladder regeneration.

This systematic review provides a comprehensive synthesis of preclinical evidence on tissue engineering strategies for bladder reconstruction, with particular focus on biomaterial design, cellularization approaches, functional outcomes, and translational potential in pediatric settings.

Materials and Methods

This systematic review was conducted in accordance with the Preferred Reporting Items for Systematic Reviews and Meta-Analyses (PRISMA) Statement (http://www.prisma-statement.org/). A comprehensive literature search was employed across PubMed, Scopus, and Embase electronic

databases, covering all records from database inception to May 2025. The search strategy combined relevant keywords and Boolean operator combinations, including "bladder" AND "reconstruction" OR "tissue engineering" OR "scaffold" OR "biomaterials" OR "stem cells" OR "urothelium" OR "smooth muscle regeneration." Additional studies were identified through manual screening of the reference lists of all eligible publications. The selection criteria were limited to original research articles published in English reporting in vitro or in vivo preclinical studies on tissue engineering approaches for bladder reconstruction. Studies were eligible if they described a bioengineered construct tested in a preclinical setting with measurable histological, molecular, or functional outcomes related to bladder regeneration. Review articles, editorials, and clinical-only studies were excluded. Data were extracted for each included study regarding:

- study type (i.e., in vitro, in vivo, or combined),
- biomaterial composition and scaffold modifications,
- cell types,
- incorporated bioactive agents,
- model used,
- histological, and functional outcomes.

Two independent reviewers (L.G. and I.P.) conducted data extraction and eligibility assessments. Discrepancies were resolved by consensus or adjudication by a third author (M.G.) who was not involved in the initial screening. A structured data extraction sheet (Microsoft Excel 2007, Redmond, WA, USA) was used to collect information on authors, article title, journal, year of publication, study design, experimental model, intervention types, cell sources, scaffold material, outcome measures, and results. Due to the heterogeneity of included studies in terms of scaffold composition, functionalization strategies, and biological endpoints, a quantitative meta-analysis was not performed. Findings were synthesized qualitatively and presented descriptively.

Results

A total of 73 studies met the inclusion criteria, comprising 19 (26.0%) *in vitro* experiments, 17 (23.3%) *in vivo* studies, and 37 (50.7%) combining both *in vitro* and *in vivo* approaches. Among the 54 *in vivo* studies, a variety of models tailored to their respective aims were considered, including rodents (n = 30; 55.6%), representing the most commonly used animal model, followed by rabbits (n = 10; 18.5%) and pigs (n = 9; 16.7%). Other less frequently used animal models included dogs [4] (n = 4; 7.4%), baboons [5] (n = 1; 1.9%), and chickens [6] (n = 1; 1.9%). One study, already included in both the rodent and pig categories, employed a combined pig and rat model [3]. Therefore, the model-

specific categories were not mutually exclusive, resulting in 55 animal-model assignments across 54 unique studies.

Natural polymeric materials were investigated for scaffold production in 45 studies (61.6%), including bladder acellular matrix (BAM) [6,7], small intestinal submucosa (SIS) [8,9], and decellularized human ureter matrix [4]. Synthetic polymers (n = 15, 20.5%) primarily involved poly(1,8-octanediol-co-citrate (POC) [10,11] and poly(carbonate urethane) urea (PCUU [12]). Hybrid scaffolds combining natural and synthetic components were reported in 13 studies (17.8%) including materials such as amniotic membrane (AM) reinforced with electrospun poly(L-lactide-co-ε-caprolactone) nanofibers [13], electrospun polycaprolactone (PCL)/chitosan (CS) nanofibrous scaffold [14].

Biochemical modifications were reported in a substantial proportion of the 73 included studies. These included the incorporation of growth factors (GFs), such as VEGF (n = 4; 5.5%), IGF-1 (n = 1; 1.4%), and bFGF (n = 3; 4.1%), surface patterning (n = 1; 1.4%) and nanoparticle-based systems (n = 4; 5.5%), including PLGA nanoparticles [15], silk fibroin microspheres [16]. Mechanical characterization of the engineered constructs was conducted in 43 studies (58.9%).

In vitro biocompatibility assays were performed in 71 studies (97.3%). These commonly included cytotoxicity testing (n = 19; 26.8%), hemocompatibility assessments (n = 1; 1.4%), and evaluations of host tissue responses (n = 38; 53.5%). *In vitro* scaffold seeding was reported in 44 studies. The seeded cell density varied, with MSCs alone used in 15 (34.1%) studies (i.e., adipose-derived stem cells, ADSCs, bone marrow-derived mesenchymal stem cells, BM-MSCs), SMCs alone in 11 (25.0%) studies, UCs alone in 13 (29.5%) studies, and co-culture systems in 5 (11.4%) studies.

All *in vivo* studies assessed urothelial regeneration (n = 54; 100%) and muscular layer formation (n = 54; 100%). Angiogenesis was evaluated in 49 studies (90.7%) and tissue integration in 45 studies (83.3%). Functional bladder capacity was assessed in 34 studies (62.9%). This parameter was frequently evaluated in natural acellular scaffolds, such as BAM grafts [17] and in functionalized BAM grafts incorporating bioactive components as VEGF [7].

Histological integration was evaluated in 54 studies (100%). Natural scaffolds (BAM [6], ureteral matrix [4]) were associated with frequent regeneration of multilayered urothelium and smooth muscle, as assessed by histological analysis. Synthetic polymer scaffolds (e.g., PCL) [18] supported epithelial layer formation *in vitro*, but less often achieved complete tissue architecture *in vivo* unless combined with natural elements. Hybrid scaffolds combining natural ECM with synthetic polymers (e.g., polyesterurethane + BAM) [19] were associated with improvements in functional bladder capacity and mechanical stability, with variation according to the proportion of the natural component. In 48 studies (88.9%), histological integration was accompanied by neovascularization

and the establishment of organized tissue architecture. Natural scaffolds have shown extensive vascularization, characterized by dense CD31-positive capillary networks and well-aligned smooth muscle bundles [7,17]. Hybrid constructs showed microvessel formation in ECM-rich regions, with limited vascular ingrowth in dense synthetic scaffolds [19,13]. In contrast, moderate angiogenesis was reported in synthetic scaffolds (i.e., electrospun PCL [18]), with increased angiogenic markers reported when combined with angiogenic GFs [18]. Inflammatory and immune responses were assessed in 29 studies (53.7%). In studies using natural ECM-based scaffolds, inflammatory cell infiltration was reported as mild and transient, with resolution within the observation period [20,17,21]. Hybrid scaffolds, as polyester urethane–BAM composites [19], were associated with moderate inflammatory responses in the early postoperative phase. Synthetic polymeric scaffolds were frequently associated with prolonged inflammatory responses characterized by macrophage and lymphocyte infiltration, with persistence over the study period. [22]

Complications were documented in 30 *in vivo* studies (55.6%). Fibrosis was frequently reported in acellular natural scaffolds [23], and degradation issues, either very rapid or delayed, were observed in synthetic scaffolds and in hybrid scaffolds, with suboptimal design parameters [22], with an unbalanced ratio between the natural ECM and synthetic component. Stone formation was a recurrent problem in natural scaffolds [21] directly exposed to urine. Urinary tract infections were rare across all scaffold types.

Clinical translation was discussed in 48 studies (88.9%), and comparisons with enterocystoplasty were reported in approximately 45% of studies.

Journal Pre-proof

Discussion

This systematic review explored the evolving landscape in preclinical bladder tissue engineering, characterized by increasing complexity in scaffold design and a growing emphasis on recapitulating the native bladder microenvironment. Importantly, when the preclinical evidence is considered as a whole, it becomes clear that no single design parameter - material origin, mechanical properties, or biological functionalization - is sufficient to achieve sustained bladder regeneration in isolation. Instead, functional success consistently emerges only when all these elements are simultaneously integrated within the same construct.

The use of decellularized extracellular matrix (ECM) components derived from collagen and glycosaminoglycans provides advantages due to their inherent bioactivity and ability to support host cell infiltration and remodeling. Various tissue sources have been explored, including porcine BAM [24,7,17], small intestinal submucosa (SIS) [8,25], ureteral matrix [4] colon matrix [20] and

pericardial matrix [26]. These substrates retain the native ECM architecture and structural proteins, providing inherent bioactivity that supposedly would support urothelial and smooth muscle regeneration. Taken together, these findings suggest that preservation of native ECM composition and ultrastructure is a key determinant of effective tissue remodeling. Sharma et al. (2022) [9] developed decellularized ECM scaffolds enriched in collagen and glycosaminoglycans and modified them with long aliphatic chains. This modification increased resistance to enzymatic degradation and physiological stability while preserving high stretchability and bladder-like compliance, thereby prolonging scaffold integrity and mechanical support during tissue remodeling. In preclinical evaluation, these constructs preserved native ECM bioactivity, representing a valuable biological platform for potential functionalization with growth factors. Nevertheless, batch-to-batch variability and inconsistent mechanical properties remain major limitations of purely natural scaffolds, posing challenges for reproducibility and clinical translation. Conversely, synthetic scaffolds, including electrospun PCL [18,27], PCUU [12], and PLCL [28], offer tailorable mechanical performance through modulation of composition and fabrication parameters, high scalability in manufacturing, and slower degradation rates compared to natural ones, which contribute to maintaining bladder compliance during the early phases of regeneration. However, evidence across studies indicates that synthetic materials alone frequently fail to achieve complete tissue integration, with reported drawbacks including chronic inflammatory responses to degradation products and limited biological interaction in the absence of surface functionalization. Depending on polymer composition and degradation kinetics, the local accumulation of acidic oligomers or particulate debris may alter tissue pH and sustain macrophage recruitment and foreign-body reactions, thereby promoting fibrosis and impairing scaffold integration. Thus, mechanical tunability alone appears insufficient to support long-term functional regeneration.

To overcome these limitations, the development of hybrid scaffolds that combine the structural integrity of synthetic polymers with the biological relevance of ECM-derived components represents a promising avenue. Across the reviewed literature, hybrid constructs most consistently achieved a balance between mechanical stability and biological integration. For example, Horst et al. (2017) [19] evaluated a hybrid scaffold composed of polyesterurethane (PEU) microfibers integrated with BAM in a rat model. The BAM component provided ECM-derived biological cues supporting host-cell infiltration and remodeling, whereas the synthetic polymer contributed mechanical stability and controlled degradation. The construct maintained structural integrity under physiological conditions, promoted ECM deposition, and elicited only a mild inflammatory response, illustrating how hybrid designs may compensate for the limitations of either component alone. Similarly, Wang et al. (2021) [29] reported that a bilayer construct combining heparin-functionalized PCL with BAM supported

adipose-derived stem cell seeding and promoted organized smooth muscle and vascular ingrowth. These findings highlight how the combination of synthetic reinforcement and biologically active ECM domains can overcome the limitations of either component alone.

Cell-based approaches, especially those utilizing MSCs, have shown consistent benefits in promoting both urothelial and muscle tissue regeneration. The paracrine effects of stem cells, particularly their secretion of trophic factors and immunomodulatory molecules, likely contributes to this enhanced regenerative capacity [30]. Importantly, the reviewed evidence suggests that regenerative efficacy depends not only on cell type but also on seeding density, spatial organization, and three-dimensional arrangement. In a preclinical study, Pokrywczynska et al. [23] (2018) seeded adipose- and bone marrow–derived MSCs onto BAM, observing that both supported smooth muscle regeneration, with higher cell seeding densities proving critical for robust outcomes. Similarly, Smolar et al. (2020) [30] combined bladder smooth muscle cells with predifferentiated ADSCs in compressed collagen hydrogels, achieving improved angiogenesis and muscle organization compared to controls. Another example is provided by Planta et al. (2024) [31], who integrated SMC spheroids into collagen scaffolds. Compared with conventional dispersed single-cell seeding, spheroid-based constructs preserve three-dimensional cell-cell interactions and endogenous extracellular matrix, which may enhance cell survival and support maintenance of the smooth muscle contractile phenotype. Accordingly, these constructs showed increased expression of contractile markers. Collectively, these studies highlight that the choice of the appropriate cell type and cell seeding strategy deeply influences scaffold biointegration, with autologous sources and 3D cell arrangements often providing the most consistent regenerative outcomes.

The integration of biological signals, including ECM-derived bioactive molecules, platelet-rich plasma (PRP)-derived GFs [26] or platelet-rich fibrin (PRF)-derived GFs [32] within the structural framework of scaffolds has emerged as a valid strategy to promote effective tissue regeneration. While pro-angiogenic factors such as VEGF, IGF-1, and bFGF consistently enhanced neovascularization, their impact on long-term functional recovery remained variable across studies, emphasizing the importance of controlled and sustained delivery rather than simple factor incorporation. Notably, the high frequency of reported angiogenesis across studies (90.7%) did not translate proportionally into improvements in bladder capacity or compliance (62.9%), indicating a dissociation between vascularization and functional recovery in current preclinical models. For example, Luevano-Colmenero et al. (2025) [26] coated decellularized bovine pericardial scaffolds with oligourethane-crosslinked ECM gels impregnated with PRP. This modification improved urothelial cell adhesion and proliferation *in vitro* and promoted angiogenesis and urothelial coverage

in vivo in a rabbit bladder augmentation model, although it did not translate in consistent functional outcomes.

In vitro studies have provided insights into scaffold performance prior to implantation [33]. For example, Wang et al. (2021) [29] evaluated a bilayer construct composed of heparin-functionalized PCL combined with BAM, showing *in vitro* sustained heparin release, enhanced proliferation and myogenic differentiation of ADSCs. Similarly, Ling et al. (2024) [34] investigated BAM-based patches incorporating a conductive GelMA–ChiNC–MXene hydrogel seeded with ADSCs, where *in vitro* assays under electrical stimulation demonstrated improved cell proliferation and metabolic activity at low voltages, while higher voltages were cytotoxic. These findings indicate that scaffolds integrating ECM components, optimized physicochemical properties, and bioactive cues provide a more favorable microenvironment for cell incorporation and functional regeneration.

In vivo animal studies have confirmed and expanded these findings. Kajbafzadeh et al. (2016) [20] implanted decellularized colon matrix in an *in vivo* rat bladder augmentation model, achieving progressive regeneration with urothelial continuity, smooth muscle and vascular ingrowth, and partial neural recovery over 9 months. Yu et al. (2022) [35] employed a pedicled vascularized construct composed of smooth muscle cell sheets combined with buccal mucosa on a capsule vascular bed in rabbits, which provided continuous mucosal coverage and preserved bladder compliance. Authors of these *in vivo* studies measured bladder capacity, compliance, histological regeneration of urothelium and muscle layers, and degree of fibrosis.

Neural recovery was less frequently investigated than urothelial, smooth muscle, and vascular regeneration. Where assessed, reinnervation was mainly evaluated histologically using neural markers such as S100/S100β, NeuN, neurofilament, βIII-tubulin, or synaptophysin, and was generally partial. Since the detection of neural markers does not necessarily demonstrate restoration of coordinated bladder function, future studies should combine histological assessment of reinnervation with functional and neurophysiological evaluations.

Evidence from both *in vitro* and *in vivo* analyses indicates the most promising scaffolds were composite constructs integrating synthetic polymer frameworks for mechanical stability with ECM-derived components for bioactivity. While many of these designs incorporated pre-seeded cells to accelerate regeneration, synthetic [36] and hybrid scaffold [13] without pre-seeded cells have also demonstrated promising outcomes, showing that well-engineered acellular constructs can effectively exploit host-driven regeneration. Adamowicz et al. (2016) [13] developed a hybrid scaffold combining amniotic membrane with electrospun PLCL nanofibers, implanted in rats. The construct supported *in vitro* urothelial regeneration and smooth muscle bundle formation with good vascularization and integration, although the regenerated wall was stiffer than native tissue.

Despite these promising advances, several key challenges persist: the variability in animal models, study duration, outcome measures, and implantation sites complicates direct comparisons across studies. Furthermore, most studies reported follow-up periods shorter than 6 months and lacked adequate functional validation in large-animal models that more closely mimic human bladder physiology, such as pigs and dogs. Additionally, only few studies address potential immunogenicity, scaffold degradation kinetics, or the risk of fibrosis and stone formation, which are crucial considerations for clinical application.

By systematically integrating material composition, biological functionalization, cellular strategies, and *in vivo* outcomes, this review clarifies that future advances in bladder tissue engineering are unlikely to arise from optimization of individual components, but rather from coordinated, system-level scaffold design.

Future research should prioritize the development of standardized protocols for scaffold fabrication, cell sourcing, and *in vivo* testing. Emphasis should also be placed on integrating advanced imaging and molecular techniques to monitor tissue integration and functional maturation longitudinally. The implementation of bioreactor systems for preconditioning tissue-engineered constructs, along with the incorporation of bioresponsive or innovative materials, may further optimize outcomes. Collaborative efforts across multidisciplinary teams encompassing biomaterials scientists, urologists, developmental biologists, and bioengineers will be essential to bridge the gap from bench to bedside.

Conclusion

Preclinical studies in bladder tissue engineering have demonstrated that durable functional regeneration does not arise from optimization of individual scaffold parameters alone, but rather from the integration of material origin, mechanical support and biological cues. Composite scaffolds combining structural stability with ECM-derived components, together with stem cell seeding and controlled delivery of bioactive factors, have shown the most consistent regenerative patterns across preclinical models. However, the frequent dissociation between angiogenesis and functional recovery underscores the need for more stringent functional validation. Future preclinical studies should also incorporate dedicated histological and functional assessment of bladder reinnervation, as the detection of neural markers alone does not establish restoration of coordinated bladder function. Long-term, standardized investigations in large animal models therefore remain essential to assess scaffold durability, safety, and true translational potential in humans.

References

[1] Atala A, Bauer SB, Soker S, Yoo JJ, Retik AB. Tissue-engineered autologous bladders for patients needing cystoplasty. Lancet. 2006;367(9518):1241-6. https://doi.org/10.1016/S0140-6736(06)68438-9

[2] Atala A. Regenerative bladder augmentation using autologous tissue-when will we get there? J Urol 2014;191:1204-5.

[3] Osborn SL, et al. Autologous regeneration of blood vessels in urinary bladder matrices provides early perfusion after transplant to the bladder. J Tissue Eng Regen Med. 2022;16(8):718-731. https://doi.org/10.1002/term.3323

[4] Sabetkish S, Sabetkish N, Kajbafzadeh A-M. Regeneration of muscular wall of the bladder using a ureter matrix graft as a scaffold. Biotech Histochem. 2021;97(3):207-214. https://doi.org/10.1080/10520295.2021.1931448

[5] Bury MI, et al. Multipotent bone marrow cell–seeded polymeric composites drive long-term, definitive urinary bladder tissue regeneration. PNAS Nexus. 2024;3(2). https://doi.org/10.1093/pnasnexus/pgae038

[6] Garriboli M, et al. Development of a porcine acellular bladder matrix for tissue-engineered bladder reconstruction. Pediatr Surg Int. 2022;38(5):665-677. https://doi.org/10.1007/s00383-022-05094-2

[7] Jiang X, et al. VEGF-loaded nanoparticle-modified BAMAs enhance angiogenesis and inhibit graft shrinkage in tissue-engineered bladder. Ann Biomed Eng. 2015;43(10):2577-2586. https://doi.org/10.1007/s10439-015-1284-9

[8] Casarin M, et al. Porcine small intestinal submucosa (SIS) as a suitable scaffold for the creation of a tissue-engineered urinary conduit: Decellularization, biomechanical and biocompatibility characterization using new approaches. Int J Mol Sci. 2022;23(5):2826. https://doi.org/10.3390/ijms23052826

[9] Sharma S, et al. Development of enzymatic-resistant and compliant decellularized extracellular matrixes via aliphatic chain modification for bladder tissue engineering. ACS Appl Mater Interfaces. 2022;14(33):37301-37315. https://doi.org/10.1021/acsami.2c06865

[10] Snow-Lisy DC, et al. The role of genetically modified mesenchymal stem cells in urinary bladder regeneration. PLoS One. 2015;10(9). https://doi.org/10.1371/journal.pone.0138643

[11] Bury MI, et al. The effects of bone marrow stem and progenitor cell seeding on urinary bladder tissue regeneration. Sci Rep. 2021;11(1). https://doi.org/10.1038/s41598-021-81939-5

Journal Pre-proof

[12] Sivaraman S, et al. Evaluation of poly (carbonate-urethane) urea (PCUU) scaffolds for urinary bladder tissue engineering. Ann Biomed Eng. 2018;47(3):891-901. https://doi.org/10.1007/s10439-018-02182-0

[13] Adamowicz J, et al. New amniotic membrane based biocomposite for future application in Reconstructive Urology. PLoS One. 2016;11(1). https://doi.org/10.1371/journal.pone.0146012

[14] Derakhshan MA, Zarchi, Harati. Electrospun PCL/chitosan nanofibrous scaffold for human bladder smooth muscle regeneration. Nanomed J. 2022;9. https://doi.org/10.22038/NMJ.2022.62927.1658

[15] Jiang X, et al. Co-delivery of VEGF and BFGF via a PLGA nanoparticle-modified BAM for effective contracture inhibition of regenerated bladder tissue in rabbits. Sci Rep. 2016;6(1). https://doi.org/10.1038/srep20784

[16] Zhao W, et al. Biomimetic multilayer scaffolds with prolonged retention of stem cells-recruiting and angiogenic peptides for promoting bladder regeneration. Compos Part B Eng. 2024;277:111409. https://doi.org/10.1016/j.compositesb.2024.111409

[17] Sabetkish S, Sabetkish N, Kajbafzadeh A-M. In-vivo regeneration of bladder muscular wall with whole decellularized bladder matrix: A novel hourglass technique for duplication of bladder volume in rabbit model. J Pediatr Surg. 2020;55(10):2226-2232. https://doi.org/10.1016/j.jpedsurg.2019.11.020

[18] Kim HY, et al. Bladder regeneration using a polycaprolactone scaffold with a gradient structure and growth factors in a partially cystectomized rat model. J Korean Med Sci. 2020;35(41). https://doi.org/10.3346/jkms.2020.35.e374

[19] Horst M, et al. Polyesterurethane and acellular matrix based hybrid biomaterial for bladder engineering. J Biomed Mater Res B Appl Biomater. 2017;105(3):658-667. https://doi.org/10.1002/jbm.b.33591

[20] Kajbafzadeh A-M, et al. In vivo regeneration of bladder muscular wall using decellularized colon matrix: An experimental study. Pediatr Surg Int. 2016;32(6):615-622. https://doi.org/10.1007/s00383-016-3871-8

[21] Estrada Mira S, et al. Use of the extracellular matrix from the porcine esophagus as a graft for bladder enlargement. J Pediatr Urol. 2019;15(5):531-545. https://doi.org/10.1016/j.jpurol.2019.07.013

[22] Rezaei H, et al. Poly-phosphate increases SMC differentiation of mesenchymal stem cells on PLGA–polyurethane nanofibrous scaffold. Cell Tissue Bank. 2020;21(3):495-505. https://doi.org/10.1007/s10561-020-09836-1

Journal Pre-proof

[23] Pokrywczynska M, et al. Understanding the role of mesenchymal stem cells in urinary bladder regeneration—a preclinical study on a porcine model. Stem Cell Res Ther. 2018;9(1). https://doi.org/10.1186/s13287-018-1070-3

[24] Yiu F, et al. Assessing the effects of bladder decellularization protocols on extracellular matrix (ECM) structure, mechanics, and biology. J Pediatr Urol. 2024;20(5):843-850. https://doi.org/10.1016/j.jpurol.2024.06.002

[25] Pokrywczynska M, et al. Does the mesenchymal stem cell source influence smooth muscle regeneration in tissue-engineered urinary bladders?. Cell Transplant. 2018;26(11):1780-1791. https://doi.org/10.1177/0963689717722787

[26] Luevano-Colmenero GH, et al. Pericardial bioscaffold coated with ECM gels and urothelial cells for the repair of a rabbit urinary bladder defect. Biomater Sci. 2025;13(7):1671-1682. https://doi.org/10.1039/d4bm00846d

[27] Naji M, et al. Experimental research supportive features of a new hybrid scaffold for Urothelium Engineering. Arch Med Sci. 2015;2:438-445. https://doi.org/10.5114/aoms.2015.50977

[28] Shrestha KR, et al. Stem cells seeded on multilayered scaffolds implanted into an injured bladder rat model improves bladder function. Tissue Eng Regen Med. 2019;16(2):201-212. https://doi.org/10.1007/s13770-019-00187-x

[29] Wang C, et al. Bladder muscle regeneration enhanced by sustainable delivery of heparin from bilayer scaffolds carrying stem cells in a rat bladder partial cystectomy model. Biomed Mater. 2021;16(3):035033. https://doi.org/10.1088/1748-605x/abf08b

[30] Smolar J, et al. Detrusor bioengineering using a cell-enriched compressed collagen hydrogel. J Biomed Mater Res B Appl Biomater. 2020;108(7):3045-3055. https://doi.org/10.1002/jbm.b.34633

[31] Planta D, et al. Smooth muscle spheroids: Superior building blocks for bladder tissue engineering. J Appl Biomater Funct Mater. 2024;22. https://doi.org/10.1177/22808000241305301

[32] Hu S, et al. The effect of platelet-rich fibrin on the biological properties of urothelial cells. Sci Rep. 2024;14(1). https://doi.org/10.1038/s41598-024-75699-1

[33] Hoogenkamp HR, et al. Scaffolds for whole organ tissue engineering: Construction and in vitro evaluation of a seamless, spherical and hollow collagen bladder construct with appendices. Acta Biomater. 2016;43:112-121. https://doi.org/10.1016/j.actbio.2016.07.022

[34] Ling Z, et al. Electrostimulation-based decellularized matrix bladder patch promotes bladder repair in rats. ACS Biomater Sci Eng. 2024;10(10):6498-6508. https://doi.org/10.1021/acsbiomaterials.4c00961

[35] Yu M, et al. Engineering pedicled vascularized bladder tissue for functional bladder defect repair. Bioeng Transl Med. 2022;8(5). https://doi.org/10.1002/btm2.10440

[36] Kini M, Bury MI, Sharma AK. An acellular platform to drive urinary bladder tissue regeneration. Adv Ther. 2024;8(1). https://doi.org/10.1002/adtp.202400158

[37] Keene JB, et al. Pre-vascularisation of the acellular bladder matrix using the omentum in a porcine model prior for bladder reconstruction—a step towards clinical application?. Pediatr Surg Int. 2024;40(1). https://doi.org/10.1007/s00383-024-05855-1

[38] Xiao D, et al. Adipose-derived stem cells-seeded bladder acellular matrix graft-silk fibroin enhances bladder reconstruction in a rat model. Oncotarget. 2017;8(49):86471-86487. https://doi.org/10.18632/oncotarget.21211

[39] Moreno-Manzano V, et al. Human adipose-derived mesenchymal stem cells accelerate decellularized neobladder regeneration. Regen Biomater. 2019;7(2):161-169. https://doi.org/10.1093/rb/rbz049

[40] Vardar E, et al. IGF-1-containing multi-layered collagen-fibrin hybrid scaffolds for bladder tissue engineering. Acta Biomater. 2016;41:75-85. https://doi.org/10.1016/j.actbio.2016.06.010

[41] Winde F, et al. Bladder augmentation using Lyoplant®: First experimental results in rats. Tissue Eng Regen Med. 2019;16(6):645-652. https://doi.org/10.1007/s13770-019-00209-8

[42] Guo H-L, et al. Bladder reconstruction using autologous smooth muscle cell sheets grafted on a pre-vascularized capsule. Theranostics. 2020;10(23):10378-10393. https://doi.org/10.7150/thno.47006

[43] Kajbafzadeh A-M, et al. Decellularized human fetal intestine as a bioscaffold for regeneration of the rabbit bladder submucosa. J Pediatr Surg. 2018;53(9):1781-1788. https://doi.org/10.1016/j.jpedsurg.2018.01.018

[44] Steins A, et al. In vitro evaluation of spider silk meshes as a potential biomaterial for bladder reconstruction. PLoS One. 2015;10(12):e0145240. https://doi.org/10.1371/journal.pone.0145240

[45] Zhao J, et al. Porous gelatin microspheres implanted with adipose mesenchymal stromal cells promote angiogenesis via protein kinase B/endothelial nitric oxide synthase signaling pathway in bladder reconstruction. Cytotherapy. 2023;25(12):1317-1330. https://doi.org/10.1016/j.jcyt.2023.08.005

[46] Ahmed MF, et al. Augmentation cystoplasty in dogs: A comparative study of different tunica vaginalis grafts. Vet Anim Sci. 2022;16:100247. https://doi.org/10.1016/j.vas.2022.100247

[47] Xiao D, et al. MicroRNA-126 from stem cell extracellular vesicles encapsulated in a tri-layer hydrogel scaffold promotes bladder angiogenesis by activating CXCR4/sdf-1α pathway. Chem Eng J. 2021;425:131624. https://doi.org/10.1016/j.cej.2021.131624

Journal Pre-proof

[48] Gerwinn T, et al. Improved contractile potential in detrusor microtissues from pediatric patients with end stage lower urinary tract dysfunction. Front Cell Dev Biol. 2022;10. https://doi.org/10.3389/fcell.2022.1007265

[49] Sabeel OM, et al. The effect of omental pedicle flap with platelets-rich fibrin on reconstruction of induced-urinary bladder defect in dogs. Iraqi J Vet Sci. 2024;38(3):543-554. https://doi.org/10.33899/ijvs.2024.145652.3386

[50] Rodrigues AF, et al. Bovine tunica albuginea conserved in honey as xenograft for Cystoplasty in rats. Cienc Rural. 2021;51(6). https://doi.org/10.1590/0103-8478cr20200501

[51] Vishwakarma SK, et al. Biofabrication of cell-laden allografts of goat urinary bladder scaffold for organ reconstruction/regeneration. Tissue Cell. 2020;67:101443. https://doi.org/10.1016/j.tice.2020.101443

[52] Wan Q, et al. Urothelium with barrier function differentiated from human urine-derived stem cells for potential use in urinary tract reconstruction. Stem Cell Res Ther. 2018;9(1). https://doi.org/10.1186/s13287-018-1035-6

[53] Leonhäuser D, et al. Potential in two types of collagen scaffolds for urological tissue engineering applications – are there differences in growth behaviour of juvenile and adult vesical cells?. J Biomater Appl. 2015;30(7):961-973. https://doi.org/10.1177/0885328215610824

[54] Kirpatovskii VI, et al. Collagen-1 membrane for replacing the bladder wall. Bull Exp Biol Med. 2016;162(1):102-106. https://doi.org/10.1007/s10517-016-3556-2

[55] Barski D, et al. Bladder reconstruction with human amniotic membrane in a xenograft rat model: A preclinical study. Int J Med Sci. 2017;14(4):310-318. https://doi.org/10.7150/ijms.18127

[56] Shi C, et al. Bladder regeneration in a canine model using a bladder acellular matrix loaded with a collagen-binding BFGF. Biomater Sci. 2017;5(12):2427-2436. https://doi.org/10.1039/c7bm00806f

[57] Leonhäuser D, et al. Two differentially structured collagen scaffolds for potential urinary bladder augmentation: Proof of concept study in a Göttingen minipig model. J Transl Med. 2017;15(1). https://doi.org/10.1186/s12967-016-1112-5

[58] Bouhout S, Tremblay J, Bolduc S. Maintenance of bladder urothelia integrity and successful urothelialization of various tissue-engineered mesenchymes in vitro. In Vitro Cell Dev Biol Anim. 2015;51(9):922-931. https://doi.org/10.1007/s11626-015-9923-x

[59] Zhou Z, et al. Intraperitoneal incubation of bladder acellular matrix grafts improves bladder smooth muscle regeneration via neovascularization. Biotechnol Bioprocess Eng. 2015;20(3):523-531. https://doi.org/10.1007/s12257-014-0705-1

Journal Pre-proof

[60] Bouhout S, Chabaud S, Bolduc S. Organ-specific matrix self-assembled by mesenchymal cells improves the normal urothelial differentiation in vitro. World J Urol. 2015;34(1):121-130. https://doi.org/10.1007/s00345-015-1596-2

[61] Jaimes-Parra BD, et al. ex vivo construction of a novel model of bioengineered bladder mucosa: A preliminary study. Int J Urol. 2015;23(1):85-92. https://doi.org/10.1111/iju.12963

[62] Hidas G, et al. Aerosol transfer of bladder urothelial and smooth muscle cells onto demucosalized colonic segments for bladder augmentation: In vivo, long term, and functional pilot study. J Pediatr Urol. 2015;11(5). https://doi.org/10.1016/j.jpurol.2015.02.020

[63] Sivaraman S, et al. Tetronic®-based composite hydrogel scaffolds seeded with rat bladder smooth muscle cells for urinary bladder tissue engineering applications. J Biomater Sci Polym Ed. 2014;26(3):196-210. https://doi.org/10.1080/09205063.2014.989482

[64] Goedegebuure M, et al. A biodegradable microgrooved and tissue mechanocompatible citrate-based scaffold improves bladder tissue regeneration. Bioact Mater. 2024;41:553-563. https://doi.org/10.1016/j.bioactmat.2024.07.030

[65] Zhao J, et al. A bilayer bioengineered patch with sequential dual-growth factor release to promote vascularization in bladder reconstruction. Regen Biomater. 2024;11. https://doi.org/10.1093/rb/rbae083

[66] Affas S, et al. Augmentation cystoplasty of diseased porcine bladders with bi-layer silk fibroin grafts. Tissue Eng Part A. 2019;25(11-12):855-866. https://doi.org/10.1089/ten.tea.2018.0113

[67] Xiao D, et al. Comparison of morphological and functional restoration between asymmetric bilayer chitosan and bladder acellular matrix graft for bladder augmentation in a rat model. RSC Adv. 2017;7(67):42579-42589. https://doi.org/10.1039/c7ra07601k

[68] Derakhshan MA, et al. Electrospun plla nanofiber scaffolds for bladder smooth muscle reconstruction. Int Urol Nephrol. 2016;48(7):1097-1104. https://doi.org/10.1007/s11255-016-1259-2

[69] Juul N, et al. Surgical implantation of single-staged tissue-engineered urothelial tubes in a minipig model. J Vis Exp [Preprint]. 2024;(209). https://doi.org/10.3791/66936

[70] Juul N, et al. Advancing autologous urothelial micrografting and composite tubular grafts for future single-staged urogenital reconstructions. Sci Rep. 2023;13(1). https://doi.org/10.1038/s41598-023-42092-3

[71] Fu Z, et al. Injectable, stretchable, toughened, bioadhesive composite hydrogel for Bladder Injury Repair. RSC Adv. 2023;13(16):10903-10913. https://doi.org/10.1039/d3ra00402c

[72] Juul N, Amoushahi M, et al. Autologous micrografting improves regeneration of tissue-engineered urinary conduits in vivo. Sci Rep. 2024;14(1). https://doi.org/10.1038/s41598-024-72876-0

[73] Wang Y, et al. Bioengineered bladder patches constructed from multilayered adipose-derived stem cell sheets for bladder regeneration. Acta Biomater. 2019;85:131-141. https://doi.org/10.1016/j.actbio.2018.12.016

[74] Xiao D, Yan H, et al. Trilayer three-dimensional hydrogel composite scaffold containing encapsulated adipose-derived stem cells promotes bladder reconstruction via SDF-1α/CXCR4 pathway. ACS Appl Mater Interfaces. 2017;9(44):38230-38241. https://doi.org/10.1021/acsami.7b10630

[75] Yudintceva N, et al. Experimental bladder regeneration using a poly-L-lactide/silk fibroin scaffold seeded with nanoparticle-labeled allogenic bone marrow stromal cells. Int J Nanomedicine. 2016;11:4521-4533. https://doi.org/10.2147/IJN.S11165

Journal Pre-proof

Author / Year	Scaffold type	Growth factors / Bioactive additions	Cell type(s)	In vitro tests & outcomes	In vivo tests & outcomes	Neural recovery / innervation	Highlights	Drawbacks
Natural scaffold								
Garriboli et al., 2022 [6]	BAM	None	None	DNA ↓ to 0.01 μg/mg; Histology: no nuclei, collagen/elastin preserved; Collagen same, GAG ↓; ↑ tensile strength & stiffness; ↑ compliance	Chicken embryo; CAM assay: ↑ vessel ingrowth (day 6 vs control)	Not assessed	Fast decell (7h) preserves structure & mechanics; ↑ strength & compliance; Maintains micro/ultrastructure	GAG loss; possible residual detergent; no mammalian in vivo data
Sabetkish et al., 2021 [4]	Decellularized human ureter matrix	None	None	Histology: preserved collagen and smooth muscle structure in ureter matrix; SEM: intact ultrastructure	Dog; ureter-matrix graft for augmentation → smooth muscle & urothelium regenerated; bladder capacity increased.	Not assessed	Ureter matrix enables organized regeneration; preserves structural integrity.	Limited sample size; the 9-month follow-up included limited functional assessment; possible species-specific results
Vardar et al., 2016 [40]	Multi-layer collagen–fibrin (CfC) hybrid scaffold, plastically compressed	IGF-1 variant (a2PI1–8-MMP-IGF-1; fibrin-binding, MMP-cleavable for controlled release)	None (hSMCs in vitro)	IGF-1 variant stably binds fibrin (>68% at 7d); retains bioactivity; hSMCs show ↑ proliferation, migration, and elongation; viability ~81% at 3d; CfC strength ↑ vs collagen (UTS +41%; modulus +39%).	Rat; HD IGF-1-CfC → robust SMC ingrowth and organization; ↑ α-SMA & SM-MHC [18]; continuous $UPK2^{+}$ urothelium; $CD31^{+}$ vessels; scaffold integrated and degraded by 4w; 85% success, 2 urinomas.	Not assessed	IGF-1 variant with MMP-sensitive release; high retention, preserved activity; promotes muscle, urothelial, and vascular regeneration; stable and suturable scaffold.	Follow-up limited to 4 weeks; no functional data; hypertrophic urothelium; outcomes beyond 6 months unknown.
Jiang et al., 2015 [7]	BAM	VEGF-loaded nanoparticles	None	Mechanical tests: burst pressure and suture retention ≈ native; histology shows preserved ECM; DNA analysis confirms effective decellularization.	Rabbit; by 4–12 wks regenerated urothelium + smooth muscle; MVD ↑ with VEGF ($p<0.01$); shrinkage ↓ to 27% vs 58% control at 12 wks; native-like contractility	Not assessed	Sustained VEGF delivery; enhanced angiogenesis; less graft contracture	Neovessels immature; some residual shrinkage; small rabbit model & graft size; occasional stones; functional outcomes beyond the 12-week follow-up were not assessed.
Sabetkish et al., 2020 [17]	BAM	None	None	DAPI: complete DNA removal; SEM: intact ECM ultrastructure; mechanical tests: tensile strength comparable to native bladder.	Rabbit; 3 mo: urothelial and muscle regeneration (↑ α-SMA, vimentin, cytokeratin, CD31, CD34); 9 mo: organized native-like muscle; Group B: fibrosis, shrinkage, graft rejection.	Neural recovery assessed by S100 immunostaining; S100-positive structures reported.	Technique prevents early urine exposure, preserving ECM and allowing host-driven recellularization; maintains structure and mechanics comparable to native bladder.	Limited to rabbit model; despite 9-month histological follow-up, long-term functional and urodynamic assessments were not performed; GAG content unreported; urine exposure caused fibrosis and graft rejection.

Journal Pre-proof

Author / Year	Scaffold type	Growth factors / Bioactive additions	Cell type(s)	In vitro tests & outcomes	In vivo tests & outcomes	Neural recovery / innervation	Highlights	Drawbacks
Smolar et al., 2020 [30]	Compressed collagen hydrogel (CC)	None	Bladder SMC; predifferentiated ADSC; co-culture	pADSC kept SMC phenotype; ↑ viability with 2–4×10^6 cells; microtissue networks by wk 3; pADSC secreted ↑ VEGF/angiogenin.	Rat; multilayered bladder wall including urothelium, detrusor, vessels; best with 4×10^6 cells; co-culture > SMC; good integration	Nerve structures were present within the regenerated bladder wall; neural recovery remained limited.	CC hydrogels biocompatible and manageable; co-culture promoted angiogenesis; regeneration quality depended on cell density.	Follow-up limited to 8 weeks in a rat partial-defect model; collagen hydrogel weak, partially strengthened by compression; outcomes beyond 6 months were not assessed.
Winde et al., 2019 [41]	Lyoplant® (bovine pericardium collagen mesh)	None	None	None	Rat; Lyoplant® integrated and remodeled into vascularized connective tissue; preserved trilaminar wall and intact urothelium.	Not assessed	Biocompatible collagen mesh remodeled into vascularized connective tissue; no major rejection	Short 6w rat model; scaffold formed connective tissue, not true muscle; non-absorbable sutures caused macrophage buildup; no functional evaluation.
Guo et al., 2020 [42]	Cell sheet (autologous SMC sheets, pre-vascularized capsule flap)	None	Autologous bladder SMCs; endothelial progenitor cells (EPCs); SMC–EPC coculture	SMC+EPC co-culture maintained phenotype; formed microcapillary networks; ↑ VEGF, bFGF, TGF-β; viable multilayer sheets with intact ECM; 6 layers showed stronger contractility than 3.	Rabbit; sheet+capsule preserved capacity/compliance with organized muscle and vascularization; sheet only led to fibrosis and shrinkage; capsule only showed partial muscle ingrowth and transient inflammation	Not assessed	Prefabricated capsule–SMC flap maintained bladder function; generated thick vascularized muscle; overcame vascularization limits of sheet-only grafts.	Multiple surgeries with long preparation; short 3 mo follow-up; small-animal model; limited bilayer evaluation; sheet thickness not fully investigated.
Kajbafzadeh et al., 2016 [20]	Decellularized colon matrix	None	None	DNA removal confirmed (H&E, DAPI); ECM preserved (SEM, collagen assays); collagen ↑, GAG maintained.	Rat; colon patch repair: 1 mo partial cell seeding; 3 mo urothelial continuity, vessels, muscle; 9 mo organized bladder wall with all layers; no stones or rejection; 3 early losses from graft leakage.	Partial nerve growth was observed at 3 months, with progressive nerve ingrowth over follow-up.	Colon ECM preserved; progressive vascular and muscle ingrowth; full-thickness regeneration by 9 mo; no mucus or colonic cell remnants.	No urodynamic evaluation; the 9-month follow-up was insufficient to assess carcinogenic risk; small healthy-animal model; no scaffold comparison.
Yu et al., 2022 [35]	Pedicled vascularized construct (SMC sheets + buccal mucosa on capsule vascular bed)	None	Smooth muscle cells (SMCs), endothelial progenitor cells (EPCs)	Cell sheets from rabbit SMCs and EPCs; EPCs formed $CD31^+$ microvessels on capsule bed (3–7d); SMCs proliferative ($Ki67^+$); BMG retained ZO-1, claudin-1, and occludin.	Rabbit; pedicled construct showed continuous mucosa, organized SM ($desmin^+$, $\alpha\text{-}SMA^+$), dense $CD31^+$ vasculature, minimal fibrosis; preserved compliance and morphology; all survived without leakage; slight, non-significant capacity decrease.	S100β-positive nerves were observed; innervation was enhanced in vivo.	First full-layer pedicled vascularized bladder construct (SMC sheets + BMG); enabled pre-implant vascularized muscle and urothelial barrier; enhanced vascularization, muscle structure, and compliance in vivo.	Small bladder patch limited by BMG size; follow-up limited to 3 months; multi-step surgery adds complexity; functional outcomes beyond 6 months were not assessed.

Journal Pre-proof

Author / Year	Scaffold type	Growth factors / Bioactive additions	Cell type(s)	In vitro tests & outcomes	In vivo tests & outcomes	Neural recovery / innervation	Highlights	Drawbacks
Kajbafzadeh et al., 2018 [43]	Decellularized human fetal intestine	None	None	Complete decellularization (H&E, SEM); ECM preserved; collagen & sGAG ↑ vs native.	Rabbit; scaffold integrated with urothelium, lamina propria, and smooth muscle; showed vascularization; 6 mo cystometry revealed normal pressures; cystography showed normal bladder shape; no infection, stones, or rejection.	Not assessed	First use of human fetal intestine as xenogeneic scaffold; high regenerative potential; formed functional bladder wall with smooth muscle and urothelium; good biocompatibility; 6 mo follow-up.	Small healthy-animal model; ethical concerns over fetal tissue use; no scaffold comparison.
Steins et al., 2015 [44]	Spider silk mesh	Optional coating (fibronectin / poly-L-lysine tested, but not required for adhesion	Human urothelial cells (HUCs)	Silk extract non-toxic; HUCs adhered within 90 min, aligned with fibers, showed high viability; SEM: multilayer coverage by day 8; qRT-PCR: slight ↓ E-cadherin; flow cytometry: basal undifferentiated phenotype maintained.	None	Not assessed	Spider silk biocompatible; supports HUC adhesion, survival, and multilayer growth; maintains undifferentiated phenotype; superior mechanical strength to Bombyx mori silk.	In vitro only; no SMC evaluation; limited scalability of native spider silk; fiber supercontraction in wet state; requires preclinical validation.
Sharma et al., 2022 [9]	Decellularized ECM (SIS, UBM, BP, BD, HD)	aliphatic chain modification (C10–C18)	hBFCs, hBECs, THP-1 monocytes	Modified dECM showed ↑ compliance and stretchability with slower degradation; ↓ cell adhesion but viable fibroblasts/epithelial cells; induced M2 macrophage shift with ↓ TNF-α and ↑ TGF-β.	Rat; subcutaneous: slower degradation, M1→M2 macrophage shift, mild collagen deposition; bladder augmentation: modified dSIS formed urothelium, lamina propria, vessels, and smooth muscle; 50% fewer bladder stones vs unmodified.	Not assessed	Transient cross-linking improved mechanical compliance and stability; supported bladder wall regeneration with reduced stone formation.	Reduced cell adhesion due to hydrophobic surface; rat model only with 16 wks follow-up; incomplete epithelial restoration.
Luevano-Colmenero et al., 2025 [26]	Decellularized pericardial ECM (bovine & porcine)	cross-linked with oligourethane + PRP impregnation	Urothelial cells	Urothelial cells showed better adhesion and proliferation on ECM gel-coated scaffolds; Live/Dead: high viability; SEM and actin staining: spindle morphology; MTT: higher metabolic activity with ECM gel or PRP vs plain pericardium.	Rabbit; full-thickness bladder repair: bM improved capacity (60–69% vs control) vs pM (18–46%); neobladder showed urothelium, dense stroma, and angiogenesis; histology: continuous urothelium with some hyperplasia; high incidence of urinary stones.	Not assessed	Pericardial ECM with ECM gel or PRP supported urothelial seeding and integration; promoted angiogenesis and urothelial coverage; bM performed better than pM.	Frequent stone formation; epithelial hyperplasia; incomplete muscle regeneration; weaker mechanics than native bladder; follow-up limited to 5 months in a rabbit model.
Planta et al., 2024 [31]	Compressed collagen scaffold	None	SMCs (2D vs 3D spheroids); ADSCs; pADSCs	3D SMC spheroids in collagen showed ↑ proliferation, uniform multilayers, and higher contractile markers vs 2D; 3D SMC/pADSC coculture ↑ smoothelin but reduced proliferation; ADSCs had minimal impact.	None	Not assessed	First collagen scaffold with SMC spheroids; 3D SMCs showed better phenotype and contractility than 2D; pADSCs viable alternative when SMCs are limited.	No in vivo validation; reduced proliferation with pADSC coculture; gene/protein levels not fully native-like; scalability and spheroid standardization remain unresolved.

Author / Year	Scaffold type	Growth factors / Bioactive additions	Cell type(s)	In vitro tests & outcomes	In vivo tests & outcomes	Neural recovery / innervation	Highlights	Drawbacks
Zhao et al., 2023 [45]	BAM	Porous gelatin microspheres (GMs) as 3D carriers	ADSCs	ADSC-GMs increased proliferation, reduced apoptosis and senescence; >90% cell viability; enhanced VEGF, PDGF-BB, and bFGF secretion; HUVEC assays showed improved migration and angiogenesis.	Rat; ADSC-GMs+BAM improved cell retention, vascularization, and muscle regeneration; enhanced bladder compliance and capacity via AKT/eNOS activation.	No nerve regeneration was observed.	3D GM culture enhances ADSC survival & paracrine effects; sustained retention on BAM; superior angiogenesis & functional recovery vs ADSCs alone.	Rat model only; 12 wks follow-up; GM fabrication and handling remain complex.
Keene et al., 2024 [37]	BAM + Pre-vascularisation with omentum	None	None	None	Pig; BAM wrapped in omentum with expander → vascularized patches; after augmentation, patches integrated, compliant, ~83% of original size; urothelium (CK7+) covered surface; neovascularization and disorganized smooth muscle ingrowth.	Not assessed	Omental pre-vascularization improved BAM patch integration and perfusion; promising step toward clinical application.	Frequent patch shrinkage; incomplete smooth muscle formation; no urodynamic data; small, heterogeneous pilot study.
Osborn et al., 2022 [3]	UBM	optional intravascular seeding with ECFCs	Endothelial colony forming cells (ECFCs), host-derived cells	ECFCs characterized and seeded on UBMs but failed to persist in vivo.	Rat and pig; rectus-preimplanted UBMs rapidly vascularized and formed smooth muscle; rrBGs retained ~90% size post-transplant vs ≤20% for UBM; showed perfused vessels, organized muscle, urothelial lining.	Nerve regeneration was observed in the rectus-regenerated bladder grafts.	Staged rectus implantation generated vascularized autologous grafts; early inosculation prevented ischemia and contraction; enabled smooth muscle regeneration; biomechanics at 3 mo matched native bladder.	ECFC seeding ineffective; rrBGs initially stiffer than native; short 3 mo follow-up; tested only in healthy bladder models.
Hu et al., 2024 [32]	PRF	None	iPSC-derived urothelial cells	iPSCs differentiated into urothelial cells (UP1a, UP1b, UP2+); PRF had a 3D fibrin structure (H&E, TEM); cells adhered to and proliferated on PRF; CCK-8 assay: proliferation increased at 72 h; Transwell assay: migration increased vs control.	None	Not assessed	PRF biocompatible with urothelial cells; promotes proliferation/migration; growth-factor reservoir; simple autologous prep.	Only in vitro; stability of the differentiated urothelial phenotype beyond the reported culture period was not assessed; PRF from rats (species difference); no in vivo validation.
Ahmed et al., 2022 [46]	Tunica vaginalis (dog allograft = DTVA; sheep xenograft = STVX; sheep decellularized ECM = STVDEM)	None	None	None	Dog; partial cystectomy + grafts; capacity—DTVA 82%, STVX 69%, STVDEM 114% baseline; STVDEM: organized urothelium/muscle/vascularization; DTVA/STVX: disorganized + inflammation/fibrosis; STVX worst: calcification, fibrosis, 2 rejections.	Not assessed	STVDEM superior regeneration of urothelium, muscle, and vessels with ↑ bladder capacity; low-cost, accessible graft.	Small dog model only; short follow-up (12 wks); no functional urodynamics; STVX poor outcomes; variability in regeneration across groups.

Journal Pre-proof

Author / Year	Scaffold type	Growth factors / Bioactive additions	Cell type(s)	In vitro tests & outcomes	In vivo tests & outcomes	Neural recovery / innervation	Highlights	Drawbacks
Yiu et al., 2024 [24]	BAM	None	None	SDS vs TT on porcine bladders; DNA removal: SDS ≥90% vs TT ~52%; Histology/SEM: SDS preserved architecture, TT disrupted; Mechanics: both ↑ stiffness, ↓ stretchability; UTS unchanged; Proteomics: SDS preserved more diverse/abundant matrisome.	None	Not assessed	SDS superior to TT in DNA clearance, architecture preservation, and matrisome retention; detergent choice critically impacts BAM quality.	No in vivo validation; only short-term mechanical/proteomic data; some collagen loss with SDS; small sample size.
Xiao et al., 2021 [47]	Tri-layer BAMG–ADA/Gel hydrogel–silk mesh (BAMG-HS)	Encapsulation of human ASC-derived extracellular vesicles (EVs) enriched in miR-126	Human ASCs (for EV isolation); HUVECs	EVs characterized (TEM, NTA, flow cytometry, WB); DNA removal confirmed; HUVECs: increased proliferation, migration, invasion, tube formation; miR-126 delivery; CXCR4/SDF-1α activation; increased VEGF.	Rat; BAMG-HS-EVs vs BAMG-HS vs sham; EV group: increased neovascularization (CD31), organized urothelium (CK+), smooth muscle (α-SMA); cystometry: preserved micturition, increased capacity/compliance, reduced fibrosis/inflammation vs BAMG-HS alone.	Partial NeuN-positive nerve regeneration was observed but remained incomplete.	EV-loaded hydrogel scaffold; enhanced angiogenesis; smooth muscle and urothelium regeneration; improved bladder function; miR-126 key via CXCR4/SDF-1α.	Only rat model, 12 wks follow-up; variability in EV content/donor dependency; scalability/standardization of EV production unresolved.
Ling et al., 2024 [34]	BAM	3D-printed GelMA–ChiNC–MXene hydrogel bioink + electrical stimulation	ADSCs	GCM hydrogels with MXene: conductive, tunable swelling/degradation; ADSCs viable (Live/Dead, CCK-8); electrical stimulation ≤400 mV increased proliferation/activity; 800 mV cytotoxic.	Rat; 40% cystectomy; BAM-GCM0.2-ADSC-ES patches: ↑ smooth muscle (57% vs 24%), ↑ vessels (13% vs 5%); restored bladder morphology, smooth wall, no stones.	Nerve area increased (1.4% vs 0.2%), although regeneration remained partial.	ADSCs + conductive hydrogel + ES: markedly improved vascular and muscle regeneration; functional bladder repair achieved.	Short follow-up (12 wks); rat model only; ES optimization required; complex bioink preparation.
Casarin et al., 2022 [8]	Porcine SIS	Novel decellularization protocol (Tergitol + sodium cholate + Benzonase); sterilization with antibiotics/antimycotics + peracetic acid	Human fibroblasts (BJ cell line)	Complete DNA removal (<50 ng/mg); collagen preserved, elastin ↓; SIS stiffer but elastic; adequate burst pressure; fibroblasts viable (Live/Dead), proliferative (WST-1), aligned along collagen fibers up to 7 days.	None	Not assessed	Eco-friendly decell/sterilization preserves ECM; SIS cytocompatible and mechanically suitable for urinary conduits.	In vitro fibroblast-only testing; elastin loss increased stiffness; no urothelial/SMC testing; no in vivo validation.

Author / Year	Scaffold type	Growth factors / Bioactive additions	Cell type(s)	In vitro tests & outcomes	In vivo tests & outcomes	Neural recovery / innervation	Highlights	Drawbacks
Gerwinn et al., 2022 [48]	3D detrusor SMC microtissues	None	Pediatric detrusor SMCs	3D microtissues viable (Calcein-AM/PI); ESLUTD SMCs in 3D lost pathological phenotype; contractile markers (α-SMA, calponin, smoothelin, MYH11) comparable to controls; ECM proteins (collagen I/III, elastin, fibronectin) similar; ECM remodeling genes (MMPs, TIMPs, TGF-β1) not significantly different.	None	Not assessed	3D microtissues restore diseased SMCs toward a normal contractile phenotype; potential autologous cell source for bladder TE; ex vivo disease model.	Only in vitro; small pediatric sample size; age difference between groups; contractile potential not functionally tested; interpatient variability.
Sabeel et al., 2024 [49]	Omental pedicle flap	PRF	None	None	Dog; partial cystectomy repaired with omentum vs omentum+PRF; both closed without leakage; PRF: ↑ granulation, ↑ angiogenesis, ↓ inflammation, more mature connective tissue at 30 d.	Not assessed	Omentum effective for closure; PRF accelerates healing, enhances vascularization, reduces inflammation.	Short follow-up (30 d); dog-only model; no functional urodynamic assessment; early adhesions; outcomes beyond 6 months were not assessed.
Rodrigues et al., 2021 [50]	Bovine tunica albuginea	Honey preservation	None	None	Rat; partial cystectomy + graft; 15 d: disorganized layers, initial muscle formation; 30 d: complete urothelialization, moderate inflammation, neovascularization; muscle regeneration limited vs controls.	Not assessed	Honey-preserved graft biocompatible, well attached, urothelial continuity by 30 d, no rejection.	Short follow-up (30 d); high rate of stones/crystals; incomplete smooth muscle organization; rat model only.
Estrada Mira et al., 2019 [21]	Porcine esophageal ECM	None	None	DNA <60 ng/mg; dsDNA <200 bp; ECM preserved (collagen, basement membrane); SEM: intact microporous structure; Ki67: ↑ urothelial proliferation.	Rat; Patch indistinguishable from bladder; complete urothelial coverage; smooth muscle fibers infiltrated ECM; neovascularization; M2 > M1 macrophages at 30 d, balanced by 60 d.	Not assessed	Esophageal ECM supported urothelium/vessel/smooth muscle regeneration; preserved basement membrane promoted urothelial integration; regenerative M2 macrophage response.	High stone incidence; muscle fibers disorganized; small rat model only; short follow-up (60 d); no functional bladder assessment.

Journal Pre-proof

Journal Pre-proof

Author / Year	Scaffold type	Growth factors / Bioactive additions	Cell type(s)	In vitro tests & outcomes	In vivo tests & outcomes	Neural recovery / innervation	Highlights	Drawbacks
Moreno-Manzano et al., 2019 [39]	BAM	None	Human ADSCs	ADSCs seeded into decellularized bladders (5 DIV); distributed in mucosa/submucosa, clustered; predominantly SMC differentiation (↑ SMA), low p63/CK7; phalloidin/PKH26 confirmed adhesion/cytoskeleton.	Rat; near-total cystectomy; ADSC-recellularized vs decellularized grafts; ADSC: stratified urothelium, organized longitudinal/transversal smooth muscle, ↑ vimentin+ connective tissue, better vascular organization (CD31+); decellularized: poor organization, urine leakage, contracture, calcifications.	S100b-positive reinnervation was observed, but the functional bladder reflex was not fully restored.	ADSCs accelerated urothelial/smooth muscle regeneration; paracrine effects key; recellularized grafts prevented leakage/contracture vs acellular controls.	Short follow-up (20 d); rat model only; few ADSCs persisted in vivo.
Vishwakarma et al., 2020 [51]	BAM	None	Human UCB-MSCs	DNA removed; collagen preserved; GAG ↓ ~50%; MSCs adhere/proliferate on BAM; Ki67+ 50–80% by d14; MTT: ↑ proliferation vs control; MSCs CD90+/CD105+/CD34−; aligned growth with Col-IV/laminin ECM.	None	Not assessed	Perfusion decellularization: ECM/mechanics preserved; goat BAM biocompatible with human UCB-MSCs; xeno-free constructs using human serum feasible.	Only in vitro; no urothelial/SMC testing; GAG loss; no in vivo validation yet.
Pokrywczynska et al., 2018 [23]	BAM	None	Autologous ADSCs	ADSCs isolated and confirmed (CD29+/CD44+/CD90+); multipotent (adipogenic/chondrogenic/osteogenic); BAM cytotoxicity (MTT, xCELLigence): none; ADSCs on BAM (7 d): viable (PKH26+, Ki67+), multilayered, migrated into scaffold; apoptosis ≤10%.	Pig; hemicystectomy + BAM vs BAM+ADSCs; both closed defects, no stones/infection; ADSC grafts: ↑ SMC (αSMA, calponin, caldesmon), ↑ angiogenesis (vWF, CD31), ↓ fibrosis; central graft under-regenerated; ADSCs low survival; repair mainly paracrine.	Nerves were incompletely restored.	ADSCs promoted muscle/vessel regeneration, reduced fibrosis; BAM ensured integration; first large-animal (pig) model with autologous ADSCs.	Central graft poorly regenerated; urothelium incompletely restored; most ADSCs lost or phagocytosed; short follow-up (3 mo).
Wan et al., 2018 [52]	SIS with USC	Urothelial-conditioned medium; EGF (30 ng/ml); SMC-conditioned medium	Urine-derived stem cells (USCs)	USCs (CD73+/CD90+/CD105+) differentiated into urothelium under UC-conditioned + dynamic culture; ↑ uroplakins (Ia, III), CK20, AE1/AE3; tight junctions (ZO-1/2, E-cadherin, cingulin); permeability ↓ 60% (FITC-dextran); TEM: intact junctions; multilayer urothelium (5–7 layers) on SIS.	None	Not assessed	USCs non-invasively harvested; efficiently differentiated into functional urothelium with barrier properties; UC-conditioned + dynamic culture optimal; multilayer urothelium formed on collagen matrices.	In vitro only; stability beyond the reported culture period was not assessed; urothelial GAG layer untested (no urine exposure); contractile function not evaluated.

Author / Year	Scaffold type	Growth factors / Bioactive additions	Cell type(s)	In vitro tests & outcomes	In vivo tests & outcomes	Neural recovery / innervation	Highlights	Drawbacks
Leonhauser et al., 2015 [53]	Collagen I/III scaffolds (OptiMaix 2D & 3D, porcine)	None	Porcine urothelial cells (UCs) & smooth muscle cells (SMCs)	Both scaffolds supported UC/SMC growth; OptiMaix 2D: UCs continuous/multilayers, SMCs on fibrous side; OptiMaix 3D: SMCs infiltrated pores, UCs partial coverage; CellTiter-Blue: higher proliferation in German Landrace vs minipigs.	None	Not assessed	USCs non-invasively harvested; efficiently differentiated into functional urothelium with barrier function; UC-conditioned + dynamic culture optimal; multilayer urothelium formed on collagen scaffolds.	In vitro only; no functional/mechanical bladder data; limited culture duration; UCs on 3D failed to form complete epithelial barrier.
Kirpatovskii et al., 2016 [54]	Type I collagen membranes (bovine vs porcine)	None	None	None	Rabbit; partial cystectomy + collagen membranes; both integrated; porcine group: ↓ inflammation, ↑ ingrowth, volume normalized by 21 d; bovine group: persistent inflammation, adhesions, reduced volume.	Not assessed	Porcine collagen membrane superior; improved integration, faster bladder recovery, reduced inflammation.	Short follow-up (21 d); rabbit model only; incomplete epithelialization; no functional/urodynamic data.
Pokrywczynska et al., 2018 [25]	SIS	None	ADSCs; BM-MSCs	MSCs (CD29+/CD44+/CD90+/CD34–/CD45–); multipotent (adipo/osteo/chondro); SEM: good SIS adhesion; high seeding (10×10^6/cm²) → dense layer vs sparse at 4×10^6/cm².	Rat; hemicystectomy + SIS (seeded/unseeded); MSC-seeded SIS: ↑ SMC bundles (α-SMM+), full urothelial regeneration, ↓ fibrosis; high-density (10×10^6) resembled native muscle; low-density/unseeded: thin, irregular fibers, fibrotic tissue.	Not assessed	ADSCs and BM-MSCs effective for SMC regeneration; high seeding density essential for robust bundles; urothelium regenerates spontaneously.	Rat model only; short follow-up (3 mo); disorganized smooth muscle layers; unclear functional recovery; many MSCs lost after urine exposure.
Hoogenkamp et al., 2016 [33]	Seamless hollow collagen bladder construct with ureter/urethra appendice	γ-irradiation sterilization; optional formaldehyde vapor crosslinking	Porcine bladder UCs & SMCs; Human UCs (hTERT-NHUCs) & SMCs	UCs formed confluent lining; SMCs infiltrated multilayers; aligned with collagen; CK7+ UCs, αSMA+ SMCs; TEM: intact junctions, cytokeratin/actin; qPCR: ↑ CK7 in UCs, ↓ αSMA in SMCs vs controls.	None	Not assessed	First seamless spherical collagen scaffold mimicking bladder; cytocompatible with human/porcine UCs & SMCs; supports luminal urothelium and muscle infiltration.	Only short-term in vitro; no urine exposure; mechanical testing limited; no in vivo validation yet.
Barski et al., 2017 [55]	Human amniotic membrane (HAM), multilayer	Cryopreserved, sterilized (peracetic acid/alcohol), sealed with fibrin glue.	None	None	Rat; partial cystectomy + HAM vs suture; HAM preserved capacity, integrated, transient inflammation, αSMA+ muscle ingrowth, urothelial coverage; controls: reduced capacity.	Not assessed	HAM durable, hypoallergenic; supported urothelium/muscle regeneration; preserved bladder capacity better than suture.	Small animal; short-term (6 wks); mild rejection (glomerulitis); small grafts (10×10 mm); limited smooth muscle regeneration.

Author / Year	Scaffold type	Growth factors / Bioactive additions	Cell type(s)	In vitro tests & outcomes	In vivo tests & outcomes	Neural recovery / innervation	Highlights	Drawbacks
Shi et al., 2017 [56]	BAM	collagen-binding basic fibroblast growth factor (CBD-bFGF)	None	CBD-bFGF bound stronger to BAM than native bFGF; sustained release ≤14 d; retained bioactivity in fibroblast proliferation.	Dog; hemicystectomy + CBD-bFGF/BAM vs BAM; CBD-bFGF/BAM: ↑ capacity (41.5 vs 28.3 mL), ↑ compliance, organized αSMA+/desmin+ muscle, mature urothelium, ↑ vWF+ vessels; BAM: fibrotic, poor muscle, low compliance.	NF-positive nerve regeneration increased with CBD-bFGF/BAM but remained incomplete.	CBD-bFGF enabled sustained delivery; enhanced muscle and vessel regeneration; improved bladder function in large-animal model.	Complex recombinant preparation; canine model only; durability beyond 6 months was not assessed.
Leonhäuser et al., 2017 [57]	Collagen type I/III scaffold (OptiMaix 2D and 3D)	None	UCs & SMCs	UCs formed confluent layer on dense side (2D); SMCs multilayer on fibrous side; in 3D, both penetrated 100 µm pores but UCs lacked barrier; PanCK+ (UCs), αSMA+ (SMCs).	Pig; both scaffolds integrated, vascularized, urothelium restored; SMCs ingrew from edges; scaffold remnants up to 32 wks; seeded vs unseeded: no major differences; 3D more fragile, enabled deeper ingrowth.	Not assessed	Both OptiMaix scaffolds biocompatible; 2D easier handling, faster epithelial closure; 3D favored muscle ingrowth; combined use potentially beneficial.	Scaffold remnants persisted >26 wks; urothelial barrier slower in 3D; seeded scaffolds not superior to unseeded; only healthy pigs, no diseased model.
Jiang et al., 2016 [15]	BAM	PLGA NPs + thermo-gel; exogenous VEGF + bFGF	None (HUVECs for cytotoxicity assays)	NPs ~288 nm, spherical (SEM/DLS); sustained VEGF/bFGF release ≤60 d; CCK-8: ↑ HUVEC proliferation; LDH: non-toxic; WB: ↑ PCNA expression.	Rabbit; hemicystectomy + BAM variants; VEGF+bFGF-BAM: ↓ contracture, ↑ CD31+/αSMA+ vessels, ↑ CK+ urothelium, ↑ αSMA+ muscle, collagen I/III near native; strips showed better ACh/KCl contractility.	Not assessed	PLGA NP-BAM enabled sustained VEGF+bFGF release; synergistically enhanced vascular, muscle, and urothelial regeneration; reduced contracture; improved bladder function.	Rabbit model only; 12-wk follow-up; complex scaffold fabrication; functional outcomes beyond 6 months were not assessed.
Bouhout et al., 2015 [58]	collagen type I hydrogel (native, acellular, or BMC-cellularized)	None	BUCs, BMCs	BMC-matrices: pseudostratified urothelium, intact junctions, uroplakin+; acellular: degenerated monolayer, ↓ uroplakin; BUC adhesion ↑1.5× with BMCs; SEM/TEM: organized microplicae/interdigitations only with BMCs.	None	Not assessed	BMCs crucial for urothelial integrity, proliferation, differentiation, and uroplakin expression.	no in vivo; short-term follow-up (≤10 d); no smooth muscle bundles.
Zhou et al., 2015 [59]	BAM	intraperitoneal incubation (pre-vascularization)	None	Histology/SEM of incubated BAMG: cell infiltration, vascular-like structures, partial ECM remodeling; non-incubated: acellular, compact fibers.	Rat; incubated vs non-incubated BAMG; both: multilayer CK+ urothelium; incubated: ↑ αSMA+ muscle, ↑ CD31+ vessels, mature SMC bundles; smoother contour; capacity ↑ ≥50% baseline; stones: 63.6% control vs 8.3% incubated.	Not assessed	Intraperitoneal incubation pre-vascularized BAMGs; enhanced muscle/vessel regeneration; reduced stones; produced more organized bladder structure.	no urodynamic evaluation; rat model only; requires staged surgery.

Author / Year	Scaffold type	Growth factors / Bioactive additions	Cell type(s)	In vitro tests & outcomes	In vivo tests & outcomes	Neural recovery / innervation	Highlights	Drawbacks
Bouhout et al., 2016 [60]	Organ-specific matrix self-assembled by BMCs	None	BUCs, BMCs, dermal fibroblasts (controls)	BMC matrices: pseudostratified urothelium, uroplakin+, CK14–, ↓ ERK; DF matrices: disorganized urothelium, CK14+, ↑ ERK; BMC ECM promoted differentiation resembling native bladder.	None	Not assessed	First organ-specific self-assembled vesical matrix; supported urothelial differentiation, suppressed hyperproliferation pathways.	Only in vitro; incomplete terminal differentiation; no in vivo validation.
Jaimes-Parra et al., 2015 [61]	Fibrin-agarose hydrogel	None	Human stromal cells, human urothelial cells	Histology: fibrin-agarose stroma with stromal cells + single epithelial layer; IF: pancytokeratin+, CK7/8+, CK13+, CK4–, filaggrin weak/–, ZO-2 ↓, uroplakin III–; TEM: immature basement membrane, hemidesmosomes, incomplete junctions; viability 96% (d7), 90% (d14).	None	Not assessed	Ex vivo bladder mucosa model mimicked native structure; high viability; potential clinical applicability.	Epithelium immature, no uroplakin III or ZO-2; only ex vivo, no in vivo validation.
Hidas et al., 2015 [62]	Seromuscular colonic tissue demucosalized	None (fibrin glue carrier only)	Porcine urothelial cells (UCs), smooth muscle cells (SMCs)	None	Pig; control colocystoplasty vs demucosalized + UCs vs + UCs+SMCs; experimental: multilayer CK7+/UPKIII+ urothelium, no colonic regrowth, minimal fibrosis; UCs+SMCs: added submucosal muscle; absorption: 10% water loss in controls vs none ($p=0.027$); urine sediment/protein ↓ ($p<0.01$).	Not assessed	Aerosol spray of UCs ± SMCs with fibrin glue repopulated colon with stable urothelium; reduced absorption/secretion vs controls; prevented colonic regrowth.	1 failed graft with fibrosis; small sample; no neurogenic bladder model; no functional contractility assays.
Synthetic scaffolds								
Bury et al., 2021 [11]	POC (poly(1,8-octamethylene citrate)	None	Human BM-MSCs + $CD34^+$ HSPCs	None	Rat; high seeding (CD34-100/MSC30) → ↑ vascularization (235 vs 179 vessels/mm², $p<0.01$), ↑ large vessels (≤5000 µm², $p<0.01$); muscle ≥45% more frequent (POC 4–5/5 vs 1/4; SIS 47–51% vs 41%); bladder capacity ≥0.9 in POC (all S−), lower in SIS (0.77–0.88 F, 0.91–1.02 M); stones frequent (22.7% F, 56.1% M), more in males; hydronephrosis linked to stone burden in SIS.	Not assessed	Systematic test of MSC/HSPC ratios on POC vs SIS; higher densities enhanced vascular/muscle growth, notably in females; POC better preserved bladder capacity; informs optimal seeding density for regeneration.	Short follow-up (10 w); high stone incidence; outcomes varied by sex/scaffold; SIS prone to contraction, reduced capacity; no validation beyond 6 months or in large-animal models.

Journal Pre-proof

Author / Year	Scaffold type	Growth factors / Bioactive additions	Cell type(s)	In vitro tests & outcomes	In vivo tests & outcomes	Neural recovery / innervation	Highlights	Drawbacks
Snow-Lisy et al., 2015 [10]	Poly(1,8-octanediol-co-citrate) (POC) scaffold	Genetic modification (Cyr61OX, Cyr61KD, Wnt5aOX)	hBM-MSCs (genetically modified)	Western blot: confirmed Cyr61/Wnt5a overexpression or knockdown; Cyr61KD and Wnt5aOX validated; Wnt5aKD non-viable.	Rat; angiogenesis: Cyr61OX/Wnt5aOX ↑ (~3×), Cyr61KD ↓; Wnt5aOX ≈ MSC+CD34$^+$ HSPCs; smooth muscle: Wnt5aOX >45%, Cyr61OX ~40%, Cyr61KD ↓25%; urothelium: Wnt5aOX 71–75 µm, Cyr61OX ~59 µm, Cyr61KD ~26 µm; function: >90% capacity, ~40 cmH_2O, slight ↓ compliance.	Nerves were present in the Cyr61OX and Wnt5aOX groups and minimal in the Cyr61KD group; Cyr61OX enhanced nerve growth.	Wnt5aOX-MSCs replicated MSC+CD34$^+$ HSPC effects (multi-lineage regeneration, stable vessels, thick urothelium); Cyr61OX enhanced angiogenesis but with abnormal vessels, less muscle; Cyr61KD impaired regeneration.	Functional improvement was mainly limited to bladder capacity; small animal model; Cyr61OX vessels leaky/tortuous; Wnt5aKD cell line not viable.
Bury et al., 2024 [5]	Synthetic poly(1,8-octamethylene-citrate-co-octanol) (PRS)	None	BM- MSCs + CD34$^+$ HSPCs	None	Baboon; CS-PRS vs CS-SIS vs ileum; CS-PRS: 64–174% capacity (24 mo), normal shape, no mucus, rare DO; CS-SIS: <100%, collagen-rich, VUR/diverticula; ileum: 38–492%, mucus, HN, DO, infections; CS-PRS: 50.6% muscle, balanced collagen, vascularized (PV ≥1.5%), 68 µm urothelium, subnative contractility; RNA-seq: fewer dysregulated genes.	βIII-tubulin-positive nerves were present but did not fully regenerate to native levels.	First large-animal (baboon) 2-year study of MSC/CD34$^+$ HSPC–seeded synthetic scaffold; CS-PRS outperformed ileum and CS-SIS in capacity recovery, architecture, vascularization, urothelium, and complications.	Limited sample size; unclear contribution of MSC vs HSPC; no neurogenic bladder model.
Zhao et al., 2024 [16]	Multilayer PCL–ODex/CMC hydrogel (sandwich)	BMHP (MSC recruitment) + VEGF-mimicking peptide (VP)	No, hBMSCs and HUVECs for in vitro testing	Sustained peptide release 28 d (extended by PCL); BMHP enhanced MSC migration; VP promoted angiogenesis; BMHP+VP synergistic.	Rabbit; RBMHP+VP: maximal MSC recruitment, vascularization, organized urothelium/SMCs; ↑ contractility (SMMHC), ↓ fibrosis; fewer stones; no systemic toxicity.	Partial synaptophysin-positive innervation was observed and remained below native levels.	Dual-functional scaffold; synergistic MSC recruitment and angiogenesis; enhanced bladder architecture, vascularization, contractility; reduced fibrosis.	Short follow-up (2 mo); partial functional recovery (contractility < native); no clinical comparison; mechanisms unclear.
Goedegebuure et al., 2024 [64]	Citrate-based POCO scaffold (smooth vs microgrooved)	None	hBM-MSCs + CD34$^+$ HSPCs	hMSCs viable; aligned on microgrooves; ↑ elongation/orientation; fibroblasts + hMSCs biocompatible (~100%)	Rat; +30% capacity, slight ↑ void frequency, normal compliance; muscle:collagen ~0.6; MG+cells: urothelium ~51 µm (uniform UPIII), ↑ vessels (2–3× unseeded, smaller); unseeded: ↓ capacity, void frequency >100%.	Nerve regeneration increased in microgrooved, cell-seeded scaffolds.	First microgrooved citrate-based scaffold; microtopography + MSC/HSPC seeding improved urothelium, muscle, vessels; function restored at 4 w.	Small-animal; short follow-up (4 w); altered vessel size; modest groove effect; unclear large-animal translation.

Journal Pre-proof

Author / Year	Scaffold type	Growth factors / Bioactive additions	Cell type(s)	In vitro tests & outcomes	In vivo tests & outcomes	Neural recovery / innervation	Highlights	Drawbacks
Zhao et al., 2024 [65]	Bilayer silk fibroin (BSF) scaffold (outer compact film + inner porous matrix)	SF microspheres enabled sequential VEGF (fast) and PDGF-BB (slow) release.	ADSCs; HUVECs	ADSCs viable (Live/Dead, CCK-8); HUVECs: ↑ migration, ↑ tube formation with VEGF+PDGF-BB; ADSCs: endothelial differentiation (↑ PECAM-1, KDR; CD31+/vWF+, Ac-LDL/UEA-1 uptake).	Rat; 50% cystectomy + BSF patch; VEGF+PDGF-BB group: smooth wall, ↑ vessel density/arterioles (αSMA+/CD31+), organized urothelium (CK+) and muscle (αSMA+).	Not assessed	Bilayer SF scaffold with sequential VEGF/PDGF-BB release enhanced vascularization, urothelium, and muscle regeneration; synergistically promoted ADSC endothelial differentiation.	Short follow-up (4 wks); small-animal model; vascular maturation and function beyond 6 months were not assessed; scaffold degradation only partial.
Rezaei et al., 2020 [22]	Electrospun PLGA/PU nanofibrous scaffold ± poly-phosphate (poly-P)	None	Human adipose-derived MSCs (AT-MSCs)	SEM: uniform nanofibers; poly-P ↑ hydrophilicity (123°→82°), elongation (32%→39%), protein adsorption, MSC adhesion/proliferation/survival (7–14 d); RT-PCR: ↑ αSMA, SM22α, Calponin1, MHC, Col-I; Col-III ↑ at d14; ICC: MHC ↑ vs PU/PLGA, TCPS.	None	Not assessed	Poly-P improved scaffold hydrophilicity, biocompatibility, and MSC-to-SMC differentiation at gene/protein level; promising for bladder muscle regeneration.	No in vivo validation; mechanism of poly-P action only inferred; short-term assays; scaffold mechanical strength slightly reduced by poly-P.
Affas et al., 2019 [66]	Bi-layer silk fibroin (BLSF) graft	None	None	None	Pig; BLSF patches augmented BOO bladders; capacity ~79%, compliance 171% baseline; neotissue: urothelium (panCK+/UP3A+), muscle (SM22α+), vessels (CD31+); residual fibrosis; partial contractility recovery.	NF200-positive nerves were present within the regenerated neotissue.	First diseased large-animal (BOO) model; BLSF scaffolds enhanced function and supported vascularized smooth muscle and urothelium.	Urothelial hyperplasia/dysplasia in severe BOO; fibrosis with ↑ collagen content; contractility below normal; only short-term follow-up (3 mo).
Shrestha et al., 2019 [28]	Multilayered PLCL (poly(L-lactide-co-ε-caprolactone)) sheets	None	Human adipose-derived stem cells (hADSCs)	PLCL nanofibers showed ECM-like morphology; hADSCs viable, proliferative, evenly distributed (SEM); resazurin: non-toxic.	Rat; PLCL+hADSCs: ↑ compliance (84% vs 38–42%), ↑ contractility (5.3 vs 2.9–3.4 g); cells layered, hADSCs → SMCs (αSMA, calponin, desmin, SM-MHC ↑; IHC/WB confirmed); TGF-β1 activated; PLCL-only: no improvement.	Not assessed	hADSC-seeded PLCL sheets enhanced compliance and contractility; showed in vivo SMC differentiation; multilayer scaffold supported integration and repair.	Short-term (4w) small-animal model; no vascular regeneration assessment; scaffold degradation beyond 6 months was not assessed; translation to clinic not yet validated.
Sivaraman et al., 2018 [12]	Poly(carbonate-urethane) urea (PCUU)	None	bladder smooth muscle cells (BSMCs)	PCUU: high extensibility (~243% elongation); porosity ↑ with stretch (38%→55%); BSMCs viable (>90%), elongated, well-distributed; cytocompatible with preserved morphology.	Rat; PCUU augmentation: capacity ↑ (1997 vs 1234 µL), void volume ↑ (815–969 vs ~527 µL); survival ↑ (66% vs 0% BOO); histology: muscle/fibroblast infiltration, SMCs surface-limited; calcium deposits and inflammation present.	Not assessed	First PCUU use in BOO rat bladder; mimicked bladder mechanics; supported BSMC viability; improved capacity and survival; promising elastomer for bladder TE.	Short follow-up (3 w); limited SMC infiltration (surface only); bladder stones; poor vascularization (5–20 µm pores); degradation and functional outcomes beyond 6 months were not assessed.

Journal Pre-proof

Author / Year	Scaffold type	Growth factors / Bioactive additions	Cell type(s)	In vitro tests & outcomes	In vivo tests & outcomes	Neural recovery / innervation	Highlights	Drawbacks
Xiao et al., 2017 [67]	Asymmetric bilayer chitosan scaffold	None	None	Scaffold morphology (SEM, μCT): bilayer chitosan more porous/flexible than BAMG; mechanical tests: ↑ elastic modulus, improved strength; no cytotoxicity data.	Rat; chitosan: smoother wall, 1.5× capacity, normal compliance; ↑ αSMA+ muscle, ↑ CD31+ vessels, multilayer CK+ urothelium, ↓ fibrosis vs BAMG; both: urothelial hyperplasia.	Nerve regeneration was limited and remained incomplete.	Bilayer chitosan scaffold outperformed BAMG in muscle regeneration, vascularization, and bladder function; promising synthetic–natural hybrid.	Rat model only; short follow-up (70 d); persistent urothelial hyperplasia; calculus formation.
Derakhshan et al., 2016 [68]	Electrospun PLLA nanofibers	None	Human bladder smooth muscle cells (hBSMCs)	PLLA nanofibers uniform, bead-free; diameters: thin 171 ± 62 nm, thick 563 ± 177 nm; hBSMCs viable (Alamar Blue), attached/spread (SEM); 48 h: scattered morphology; 30 d: elongated/aligned; thick fibers enabled partial infiltration, thin more compact.	None	Not assessed	Random PLLA nanofibers induced hBSMC alignment over time; biocompatible, supported viability and SMC morphology; promising for bladder muscle TE.	Only in vitro; no urothelial component; no mechanical/functional testing; limited infiltration in dense nanofibers; no in vivo validation.
Naji et al., 2015 [27]	Electrospun PCL/PLLA (60:40) hybrid nanofibrous scaffold (oxygen plasma–treated)	None (surface oxygen plasma treatment only, to increase hydrophilicity)	Urothelial cells (in vitro only)	Nanofibers 120–1500 nm; porous, uniform, plasma-treated hydrophilic (134°→80°); SEM showed even cells, normal colonies; H&E continuous layer by 7 d; IHC panCK^{+}, UPKIII^{+}; MTT non-toxic, proliferation ↑ d1–14.	None	Not assessed	Novel PCL/PLLA nanoscaffold supported urothelial adhesion, proliferation, phenotype maintenance; biocompatible, non-toxic; promising for bladder urothelium engineering.	Only in vitro; no smooth muscle/urothelial co-culture; no in vivo validation; scaffold mechanics not tested under urine exposure.
Kini et al., 2024 [36]	Synthetic PRS (poly(1,8-octamethylene-citrate-co-octanol)) scaffold	None	None	None	Rat; TCM: muscle/collagen 52% vs 34%; urothelium 76 vs 50 μm; vascularization 2.4% vs 1.1% with larger vessels; compliance 0.71 vs 0.51; capacity 972 vs 868 μL; recovery 108% vs 91%; no stones or kidney damage.	Nerve-related measures increased (41 vs 25 μm; 1000 vs 461 μm).	First demonstration of acellular intravesical TCM therapy with synthetic PRS; promoted urothelial, muscle, and vascular regeneration; improved compliance and capacity without cell seeding.	Short follow-up (4w); small sample size (n=9); only rat model; safety and efficacy beyond 6 months were not assessed.

Journal Pre-proof

Journal Pre-proof

Author / Year	Scaffold type	Growth factors / Bioactive additions	Cell type(s)	In vitro tests & outcomes	In vivo tests & outcomes	Neural recovery / innervation	Highlights	Drawbacks
Kim et al., 2020 [18]	Polycaprolactone (PCL) scaffold with gradient pore structure	VEGF + EGF + bFGF	None	GF loading (ELISA): EGF ~39 ng, VEGF ~26 ng, bFGF ~9 ng per sheet; sustained release for 24 d without burst.	Rat; bladder volume: GF 1330–1700 µL, scaffold 907–1291 µL, cystectomy 270–573 µL; histology: GF multilayer urothelium, dense SM, ↑ angiogenesis, tighter stroma, ↓ inflammation; IHC: ↑ αSMA, panCK, ↓ CD8; genes: ↑ MyoD, desmin, myosin, αSMA, UPK1a/b/2, CK13/18/19, panCK; safety: normal at 6 mo, no toxicity; stones ~30% (scaffold & GF).	α-Bungarotoxin staining was increased, indicating enhanced neuromuscular junction formation.	Gradient PCL scaffold + GFs enabled functional and histological bladder regeneration; enhanced urothelium, muscle, angiogenesis; safe up to 6 mo.	Stone formation (~30%); short–mid term rat model (≤6 mo); incomplete degradation at 12 w; no large-animal validation.
Hybrid scaffold								
Adamowicz et al., 2016 [13]	Amniotic membrane (Am) reinforced with electrospun PLCL nanofibers (sandwich)	None	None (bone marrow MSCs for in vitro seeding)	MSCs viable on PLCL; migrated toward Am; deeply infiltrated PLCL; Am extracts non-cytotoxic (MTT, RTCA); MSCs colonized Am surface.	Rat; grafts integrated without leakage; well vascularized; multilayer hyperplastic urothelium; smoothelin^{+} muscle bundles (contractile); smooth muscle 18–41% (vs ~42% control); mild–moderate inflammation; PLCL degraded in 8–10 w; Young's modulus ↑ vs native (fibrosis-related stiffness).	Not assessed	Novel Am–PLCL biocomposite preserved Am bioactivity, added strength; supported urothelium and muscle regeneration; integrated well, no rupture or leakage.	Regenerated wall stiffer than native (fibrosis, irregular SM); muscle disorganized vs controls; small-animal only; no urodynamic data.
Juul et al., 2024 [69]	Collagen hydrogel + biodegradable mesh/stent + autologous urothelial micrografts	None	None (micrografts only)	None	Pig; conduit patent, no rejection/infection; lumen lined by stratified urothelium; mesh/stent remnants present; no strictures or obstruction at 6 w; normal behavior restored.	Not assessed	Single-stage collagen-based tubular scaffold with perioperative autologous micrografting; achieved epithelialization and patency without cell culture or ex vivo expansion.	Short follow-up (6 w); scaffold thickness may hinder nutrient diffusion; distal conduit ligated (no functional stoma); scalability and function beyond 6 months were not assessed.
Derakhshan et al., 2022 [14]	Electrospun PCL/chitosan (CS) nanofibrous scaffold	None	Human bladder smooth muscle cells (hBSMCs)	Nanofibers ~92–118 nm, smooth, defect-free; FT-IR/CHN confirmed CS incorporation; hBSMCs αSMA^{+}, elongated; SEM: good attachment, focal adhesions; Alamar Blue: viability ↑ on PCL/CS vs PCL (7 d); non-toxic; limited infiltration (dense mats).	None	Not assessed	PCL/CS blend enhanced hydrophilicity and adhesion vs PCL; supported hBSMC viability, proliferation, and morphology; suitable for bladder SMC engineering.	Only in vitro; no mechanical testing; no urothelium component; no in vivo validation.

Journal Pre-proof

Author / Year	Scaffold type	Growth factors / Bioactive additions	Cell type(s)	In vitro tests & outcomes	In vivo tests & outcomes	Neural recovery / innervation	Highlights	Drawbacks
Juul et al., 2023 [70]	Compressed collagen scaffold reinforced with Vicryl® mesh + stent	None	Porcine urothelial micrografts; human urothelial cells (bladder washing)	High-density collagen (80%) reduced permeability, improved barrier; urothelial micrografts formed multilayer urothelium with collagen IV basement membrane and uroplakin II; wash cells stratified similarly; reinforced scaffold stronger than native urethra initially, degraded over 4 w.	Pig; tubular collagen–mesh–stent conduit with autologous micrografts implanted successfully; rapid recovery, no infection/rejection; multilayer differentiated urothelium along 5-cm conduit.	Not assessed	First intraoperative collagen–mesh scaffold with urothelial micrografts assembled intraoperatively; single-stage, supported multilayer urothelium and integration.	Only short-term (3 wks); single pilot pig; conduit not connected to skin (stenosis risk unassessed); partial collagen delamination in vitro; scalability and long-term function unknown.
Fu et al., 2023 [71]	Injectable composite hydrogel (GelMA + SilMA + F127DA)	None	None	Injectable hydrogel UV-crosslinked in 90 s; pores 28–308 μm; swelling ↓ (GSF 287%); tunable degradation (22% remaining at 48 h); tensile strain ~126–148%, toughness ↑ (15→46 kJ/m³); compressive strength ↑ (≤127 kPa); fatigue-resistant, self-recovering; ADSC viability >80% (5 d); fibroblast migration ↑ (GelMA/SilMA); adhesion ↑ (31 kPa, ~95% > GS/GF); burst pressure ↑ (32 vs 21 kPa); effective ex vivo bladder sealing.	None	Not assessed	Novel injectable photo-crosslinkable hydrogel with strong mechanical, adhesive, and sealing properties; biocompatible; effective ex vivo bladder closure; promising sutureless repair material.	No in vivo validation; short-term ex vivo only; F127DA slightly ↓ proliferation; stability beyond the ex vivo observation period was not assessed.
Juul et al., 2024 [72]	Collagen scaffold reinforced with Vicryl® mesh + biodegradable stent	None	Autologous urothelial micrografts (peri-operative seeding)	None	Pig; tubular conduits implanted; micrografted: ↑ Up2+ epithelialization, ↑ Ki67, ↓ TUNEL apoptosis, ↑ Cd31 vascularization vs acellular; all conduits patent, no strictures.	Not assessed	One-stage scaffold with autologous micrografts feasible; enhanced urothelial coverage, proliferation, and vascularization vs acellular conduits; simple perioperative approach.	Short-term (6 w); small pilot; conduits not skin-connected (stenosis untested); variable distal epithelialization; mesh/stent remnants at 6 w.
Wang et al., 2019 [73]	PGA scaffold + multilayer ASC sheets	None	adipose-derived stem cells (ASCs)	USPIO labeling ≤25 μg/mL caused minimal cytotoxicity; ASCs maintained viability/proliferation; formed multilayer sheets with intact ECM/junctions; adhered firmly to PGA; MRI signal dose-dependent.	Rat; ASC patch: capacity ↑ to 152%, compliance restored by 8 w; multilayer urothelium, organized muscle, $CD31^{+}$ vessels (diameter ↑); PGA degraded by 8 w; MRI tracking up to 8 w; controls: thin urothelium, disorganized muscle, fewer vessels, no labeled cells.	NeuN-positive neurons were present but remained below control levels; innervation was partial and incomplete.	First multilayer ASC sheet–scaffold patch for bladder regeneration; preserved ECM/junctions; enabled MRI tracking (USPIO); enhanced urothelium, muscle, vessels; improved capacity and compliance.	Short-term follow-up (8w); no direct scaffold-only comparison; small-animal model only.

Author / Year	Scaffold type	Growth factors / Bioactive additions	Cell type(s)	In vitro tests & outcomes	In vivo tests & outcomes	Neural recovery / innervation	Highlights	Drawbacks
Wang et al., 2021 [29]	coaxial electrospun heparin–PCL/BAM (Hep-PB) membrane + 3D-printed PCL layer	Heparin (sustained release from Hep-PB fibers)	Adipose-derived stem cells (ADSCs)	Hep-PB/PCL scaffold supported greater ADSC proliferation vs PCL; cells became spindle-like; ↑ αSMA, SM22, calponin, MHC; collagen I/III ratio near native; sustained heparin release (~15 μg/mL, 4 w).	Rat; ASHP (ADSC + Hep-PB/PCL): smooth regenerated tissue, bladder size ~native; no leakage/contracture (cystography); histology: organized SM > collagen; ECM remodeling better than BAM/suture.	Not assessed	Combined electrospinning and 3D printing; sustained heparin release enhanced ADSC myogenic differentiation; bilayer scaffold improved bladder regeneration vs BAM and suture.	Short-term (4w) rat model; small sample size; limited functional assays; no validation beyond 6 months or in large-animal models.
Horst et al., 2017 [19]	Electrospun polyesterurethane (PEU, DegraPol) microfibers on BAM	None	Rat bladder smooth muscle cells (SMCs) and non -seeded (both tested)	SMCs attached and proliferated on PEU and PLGA hybrids; metabolic activity stable; no significant differences between polymers.	Rat; PEU-hybrid: no shrinkage, multilayer wall, continuous urothelium, SMC bundles, less inflammation, histology ↑ 4→8 w; PLGA-hybrid: shrinkage, atrophic urothelium, sparse SMCs, more inflammation, histology ↓; cystometry: 4 w capacity ↑ in PLGA, all ↓ by 8 w; compliance lowest in unseeded PEU, improved with seeding; stones in 66% (87% PEU, 44% PLGA), small/non-obstructive.	Not assessed	First PEU (DegraPol) use in bladder TE; elasticity near native; BAM hybrid supported urothelium/muscle regeneration; less inflammation and contraction vs PLGA.	Small animal (rat); short follow-up (8w); high stone incidence; bladder compliance suboptimal; no functional validation beyond 6 months.
Xiao et al., 2017 [74]	Trilayer BAMG–ADA/Gel hydrogel–silk mesh (BAMG-HS) with encapsulated ASCs	None	Adipose-derived stem cells (ASCs)	Scaffold: waterproof BAMG + ADA/Gel hydrogel + silk mesh; elastic modulus 5.3 MPa, load 28.9 N; ASCs viability >94% (7 d), proliferation ~Matrigel; uniform 3D cell distribution.	Rat; BAMG-HS+ASCs: faster hydrogel degradation, ↓ fibrosis/inflammation, minimal shrinkage; multilayer urothelium, organized SM, ↑ angiogenesis; capacity/compliance ↑ vs acellular, near control; SDF-1α/CXCR4–ERK1/2 pathway; few ASCs endothelial.	Innervation increased in the ASC-seeded constructs.	Innovative trilayer "sandwich" scaffold; encapsulated ASCs survived and promoted regeneration; enhanced urothelium, SM, vessels; improved compliance/capacity; angiogenesis mainly paracrine.	Rat model only; short-term (12w); vessel immaturity (smaller diameter); calculi formation not fully prevented; validation beyond 6 months and in large-animal models is needed.
Yudintceva et al., 2016 [75]	Bilayer poly-L-lactide/silk fibroin (PL-SF) scaffold	None	BMSCs; SPION-labeled	SPION uptake high, non-toxic; BMSCs viability/proliferation unchanged (Trypan Blue, MTT); normal morphology; SEM: multilayer growth on PL-SF; confocal: SPIONs in cytoplasm.	Rabbit; PL-SF+BMSCs: integrated scaffold, full-thickness regeneration (urothelium, SM, vessels, adventitia); urothelium ~90 μm ≈ control; vessel density ↑ (8 vs 3/mm²), diameter ↑ (96 vs 53 μm); MRI tracked BMSCs to 12 w; acellular PL-SF: 2/6 rejection, lymphocytic infiltration, disorganized tissue.	EMG activity was present, providing functional evidence of neuromuscular recovery.	PL-SF scaffold + BMSCs supported functional bladder wall regeneration with urothelium, SM, and vascularization; scaffold fully degraded; SPIONs enabled noninvasive tracking.	Short follow-up (12w); partial rejection in acellular controls; edema/collagen deposition noted; small-animal model only.

Journal Pre-proof

Author / Year	Scaffold type	Growth factors / Bioactive additions	Cell type(s)	In vitro tests & outcomes	In vivo tests & outcomes	Neural recovery / innervation	Highlights	Drawbacks
Xiao et al., 2017 [38]	Bilayer BAM + Silk Fibroin (SF)	None	ASCs	Bilayer scaffold: BAMG waterproof layer, SF porous 3D (~1.5 mm); SEM: ASCs adhered, spread, proliferated in SF; CCK-8: non-toxic, supported growth; mechanical tests: modulus ~12 MPa, load ~5.5 N; unaffected by seeding.	Rat; BAMG-SF-ASCs vs BAMG-SF vs cystotomy; ASCs: ↓ shrinkage, ↑ CK+ urothelium, ↑ αSMA+ muscle, ↑ CD31+ vessels; scaffold degraded with tissue ingrowth; ↑ SDF-1α/CXCR4/VEGF/VEGFR2, ↑ ERK1/2; capacity 224% control, ↑ compliance, voiding near normal.	NeuN-positive nerves increased, indicating enhanced innervation.	BAMG-SF scaffold effectively delivered ASCs; enhanced angiogenesis, muscle, and urothelium via SDF-1α/CXCR4/ERK1/2–VEGF pathway; improved morphology and function vs acellular BAMG-SF.	rat model only; follow-up 12 wks; calculi formation; persistent urothelial hyperplasia.
Sivaraman et al., 2015 [63]	Composite hydrogel (Tetronic® T1107-acrylate + collagen type I + hyaluronic acid)	None	bladder smooth muscle cells (BSMCs; encapsulated)	Hydrogels with 0.1–0.2% HA: swelling unchanged, stiffness ↑ with HA; BSMCs viable >90% (4–14 d); confocal: uniform, migrated, spread morphology (14 d); mechanical tests: seeded gels stronger/stiffer (11.6 vs 4.1 kPa; 42.7 vs 11.8 kPa, 14 d); collagen ↑ (62 vs 35 µg/mg).	None	Not assessed	Hybrid semi-IPN hydrogel supported BSMC survival, spreading, and collagen deposition; cells enhanced mechanical strength over time; promising for bladder regeneration.	Only short-term in vitro; no urothelial layer tested; strength still << native bladder (~100 kPa); no in vivo validation.

Table I. Summary of preclinical bladder tissue engineering studies included in the review. For each study, the scaffold type, bioactive modifications (growth factors or other additions), seeded cell type(s), *in vitro* and *in vivo* experimental designs with key outcomes, and the main highlights and drawbacks were reported. Abbreviations: BAM = Bladder Acellular Matrix; CAM = Chorioallantoic Membrane; SEM = Scanning Electron Microscopy; CfC = Collagen–fibrin Composite; IGF-1 = Insulin-like Growth Factor 1; MMP = Matrix Metalloproteinase; IGF-1R = Insulin-like Growth Factor 1 Receptor; hSMCs = Human Smooth Muscle Cells; UTS = Ultimate Tensile Strength; HD = High Dose; LD = Low Dose; SMC = Smooth Muscle Cell; α-SMA = Alpha–Smooth Muscle Actin; SM-MHC = Smooth Muscle Myosin Heavy Chain; UPK2 = Uroplakin 2; CD31 = Cluster of Differentiation 31; VEGF = Vascular Endothelial Growth Factor; MVD = Microvessel Density; DAPI = 4′,6-Diamidino-2-Phenylindole; IHC = Immunohistochemistry; ADSC = Adipose-Derived Stem Cell; pADSC = Predifferentiated Adipose-Derived Stem Cell; EPC = Endothelial Progenitor Cell; bFGF = Basic Fibroblast Growth Factor; TGF-β = Transforming Growth Factor Beta; SM = Smooth Muscle; ZO-1 = Zonula Occludens-1; BMG = Buccal Mucosa Graft; S100β = S100 Calcium-Binding Protein Beta; H&E = Hematoxylin & Eosin; sGAG = Sulfated Glycosaminoglycans; HAM = Human Amniotic Membrane; HUCs = Human Urothelial Cells; qRT-PCR = Quantitative Reverse Transcription Polymerase Chain Reaction; E-cadherin = Epithelial Cadherin; TNF-α = Tumor Necrosis Factor Alpha; PRP = Platelet-Rich Plasma; bM = Bovine

Matrix; pM = Porcine Matrix; GMs = Gelatin Microspheres; PDGF-BB = Platelet-Derived Growth Factor-BB; HUVEC = Human Umbilical Vein Endothelial Cell; AKT = Protein Kinase B; eNOS = Endothelial Nitric Oxide Synthase; Vicryl® = Polyglactin 910 Mesh; CK = Cytokeratin; CK7 = Cytokeratin 7; ECFC = Endothelial Colony-Forming Cell; rrBG = Rectus-Regenerated Bladder Graft; iPSC = Induced Pluripotent Stem Cell; UP1a/UP1b/UP2 = Uroplakin 1a/1b/2; PRF = Platelet-Rich Fibrin; DTVA = Dog Tunica Vaginalis Allograft; STVX = Sheep Tunica Vaginalis Xenograft; STVDEM = Sheep Tunica Vaginalis Decellularized Extracellular Matrix; SDS = Sodium Dodecyl Sulfate; TT = Trypsin–Triton; BAMG = Bladder Acellular Matrix Graft; ADA = Alginate Dialdehyde; EVs = Extracellular Vesicles; TEM = Transmission Electron Microscopy; NTA = Nanoparticle Tracking Analysis; WB = Western Blot; CXCR4 = C-X-C Chemokine Receptor Type 4; SDF-1α = Stromal Cell-Derived Factor 1 Alpha; NeuN = Neuronal Nuclei Marker; BSF = Bilayer Silk Fibroin; PECAM-1 = Platelet Endothelial Cell Adhesion Molecule 1; KDR = Kinase Insert Domain Receptor (VEGFR2); vWF = von Willebrand Factor; UEA-1 = Ulex Europaeus Agglutinin I; GelMA = Gelatin Methacrylate; ChiNC = Chitosan Nanocrystal; MXene = Two-Dimensional Transition Metal Carbide/Nitride Material; GCM = GelMA–ChiNC–MXene Hydrogel; ES = Electrical Stimulation; PGP9.5 = Protein Gene Product 9.5; BJ = Human Fibroblast Cell Line; WST-1 = Water-Soluble Tetrazolium-1 Assay; Tergitol = Nonionic Surfactant; TIMPs = Tissue Inhibitors of Metalloproteinases; ESLUTD = End-Stage Lower Urinary Tract Dysfunction; MYH11 = Myosin Heavy Chain 11; FT-IR = Fourier-Transform Infrared Spectroscopy; CHN = Carbon–Hydrogen–Nitrogen Analysis; F127DA = Poloxamer F127 Diacrylate; PGA = Polyglycolic Acid; USPIO = Ultrasmall Superparamagnetic Iron Oxide; MRI = Magnetic Resonance Imaging; Hep = Heparin; PLGA = Poly(lactic-co-glycolic acid); ASHP = ADSC + Heparin–PCL/BAM Construct; DegraPol = Biodegradable Polyesterurethane; SPION = Superparamagnetic Iron Oxide Nanoparticle; EMG = Electromyography; HA = Hyaluronic Acid; IPN = Interpenetrating Polymer Network; POC = Poly(1,8-octanediol-co-citrate); Cyr61 = Cysteine-Rich Angiogenic Inducer 61; Wnt5a = Wingless-Type MMTV Integration Site Family, Member 5A; OX = Overexpression; KD = Knockdown; PRS = Poly(1,8-octamethylene-citrate-co-octanol) Scaffold; BM-MSC = Bone Marrow-Derived Mesenchymal Stem Cell; HSPC = Hematopoietic Stem and Progenitor Cell; BMHP = Bone Marrow Homing Peptide; VP = VEGF-Mimicking Peptide; PU = Polyurethane; poly-P = Polyphosphate; AT-MSC = Adipose Tissue-Derived Mesenchymal Stem Cell; PLCL = Poly(L-lactide-co-ε-caprolactone); TGF-β1 = Transforming Growth Factor Beta 1; PCUU = Poly(carbonate-urethane) urea; BOO = Bladder Outlet Obstruction; PLLA = Poly(L-lactic acid); hBSMC = Human Bladder Smooth Muscle Cell; PCL = Polycaprolactone; USC = Urine-Derived Stem Cell; EGF = Epidermal Growth Factor; AE1/AE3 = Cytokeratin Antibodies AE1 and AE3; μCT = Micro-Computed Tomography; Am = Amniotic Membrane; RTCA = Real-Time Cell

Journal Pre-proof

Analysis; NF = Neurofilament; NF200 = Neurofilament 200 kDa; SM22α = Smooth Muscle Protein 22 Alpha; UP3A = Uroplakin 3A; TCM = Tissue Conditioning Medium.

Journal Pre-proof

Journal Pre-proof

Advances in preclinical tissue engineering strategies for bladder reconstruction: a systematic review.

Laura Giacomel[1], Irene Paraboschi[1,2*], Ugo Maria Pierucci[1], Michela Marinaro[1], Marco Paciotti[3,4], Vittorio Fasulo[3,4], Giovanni Lughezzani[3,4], Massimo Garriboli[5], Nicolò Maria Buffi[3,4], Silvia Farè[6], Gloria Pelizzo[1,2].

1. Department of Pediatric Surgery, "Vittore Buzzi" Children's Hospital, Milano, Italy
2. Department of Biomedical and Clinical Science, University of Milano, Milano, Italy
3. Department of Urology, IRCCS Humanitas Research Hospital, Milano, Italy
4. Department of Biomedical Sciences, Humanitas University, Milano, Italy
5. Department of Paediatric Nephro-Urology, Evelina London Children's Hospital, Guy's and St. Thomas' NHS Foundation Trust, Westminster Bridge Rd, London, United Kingdom
6. Department of Chemistry Materials and Chemical Engineering, Politecnico di Milano, Milan, Italy

The authors declare that they have no conflicts of interest.

Journal Pre-proof